LEACHABILITY OF IRON IN CEMENT WITH RICE HUSK ASH (RHA) USING WHOLE BLOCK LEACHING

POON WAI KEONG

A project report submitted in partial fulfilment of the requirements for the award of Bachelor of Engineering (Hons.) Chemical Engineering

**Lee Kong Chian Faculty of Engineering and Science
Universiti Tunku Abdul Rahman**

September 2017

DECLARATION

I hereby declare that this project report is based on my original work except for citations and quotations which have been duly acknowledged. I also declare that it has not been previously and concurrently submitted for any other degree or award at UTAR or other institutions.

Signature : _POON WAI KEONG_

Name : POON WAI KEONG

ID No. : 13UEB07517

Date : 28th August 2017

APPROVAL FOR SUBMISSION

I certify that this project report entitled **"LEACHABILITY OF IRON IN CEMENT WITH RICE HUSK ASH (RHA) USING WHOLE BLOCK LEACHING"** was prepared by **POON WAI KEONG** has met the required standard for submission in partial fulfilment of the requirements for the award of Bachelor of Engineering (Hons.) Chemical Engineering at Universiti Tunku Abdul Rahman.

Approved by,

Signature   :   _____

Supervisor   :   DR TEE SHIAU FOON

Date   :   28th August 2017

Signature   :   _____

Co-Supervisor : DR TIOH NGEE HENG

Date   :   28th August 2017

ACKNOWLEDGEMENTS

"In the middle of difficulty lies opportunity"

— Albert Einstein

ABSTRACT

Substantial urbanization upheld the anthropogenic emission of toxic wastes in the industrialized world, hence illegal practice of disposal necessitates the exploration of an economical remediation technology. Solidification/Stabilization treatment (S/S) conventionally applicable to an extensive range of radioactive wastes, preferentially favourable to an alteration in both physical and chemical aspects of hazardous contaminants. A study is undertaken to ascertain the fixation mechanism of ferric species in a cementitious system by Whole Block Leaching Procedure (WBL). Ordinary Portland Cement (OPC) accustomed as an essential binder, likewise complementary pozzolanic rice husk ash (RHA) ameliorated the effectiveness of S/S treatment. In this study, acetic acid solution (pH 2.88) stimulated the hydrologic environment as an effort to justify the leachability effects upon quantitative co-relation among distinct concentration in the extent of stipulated duration. Irregular topography of SEM signified the deterioration of matrix, primarily vulnerable to an initial ingression of acetous medium. Relative abundance of calcium hydroxide, $Ca(OH)_2$ distinguished crystallography of constituents upon successive depletion of calcium silicate (CS), correspondingly characterization of deposited solids validated the existence of calcium carbonate ($CaCO_3$) as construed in XRD. Moreover, EDX authenticated the adsorption of amorphous ferric hydroxide, $Fe(OH)_3$ by virtue of hydroxylation in the interstitial phase. Quantitative determination of ICP-OES expressed the maximal concentration of ferric upon 14 hours, moreover calcium ions accounted for 24 hours. This principle elucidated that mobility of ferric species attributed to a local pH dependency, comparably alkalinity of produced solvent likely to instigate a limited extent of leaching at the latter times. Availability of RHA alleviated hydraulic conductivity upon extensive synthesis of calcium-silicate-hydrate (C-S-H), alternatively sufficed the penetrability factor of matrix. S/S technique exhibited feasibility of disposal via a cost-effective alternative, reliably optimized the elimination of heavy metals. In a nutshell, leachability limit of ferric as below of 5 mg/L indeed satisfied the regulatory limit as adherence to "A Guide For Investor".

TABLE OF CONTENTS

LIST OF TABLES

LIST OF FIGURES

LIST OF SYMBOLS / ABBREVIATIONS

C_o	Initial Concentration, M
K	Equilibrium Constant
ppm	Part per Million
w/b	Water-to-Binder Ratio
CH	Calcium Hydroxide
CS	Calcium Silicate
C-S-H	Calcium Silicate Hydrate
EDX	Energy Dispersive X-Ray Spectroscopy
Fe (II)	Ferrous Iron
Fe (III)	Ferric Iron
ICP-AES	Inductively Couple Plasma-Atomic Emission Spectroscopy
ICP-OES	Inductive Coupled Plasma Optical Emission Spectroscopy
OPC	Ordinary Portland Cement
RHA	Rice Husk Ash
S/S	Stabilization/Solidification
SEM	Scanning Electron Microscopy
TCLP	Toxicity Characteristic Leaching Procedure
WBL	Whole Block Leaching
XRD	X-Ray Diffractogram

LIST OF APPENDICES

CHAPTER 1

INTRODUCTION

1.1   Background

In the late 18th century, industrial revolution substantially ameliorated the condition of living standards by heightening civilization. Indeed, advancement of human organization as a result of civilization enhances the production yield by developing various indispensable inventions and discoveries. For instance, machinery tools for agricultural harvesting, basic machines as well as transportation. These new inventions eventually discharge massive scale of waste, albeit bulk quantities of yield being manufactured continuously. Correspondingly, discarding used commercial products as waste into the environment, adversely leading causes of unprecedented toxic accumulation in nature. In response to the intensive growth of population, subsequently give rise to an excessive demand for resources (Jan De Vries, 1994). Hence, people are encouraged to seek for more promising alternatives in the account of resources depletion. According to statistical charts, approximately 250 million tons of waste is produced day by day, without concerning the intention of hazardous waste generation. Generation of waste has been reported to be increased exponentially since the year 1960 to 2013 (Bobby, 2014).

Occurrence of numerous catastrophic incidents have been reported in accordance to poor management skills in handling waste disposal. For example, Minamata disease was discovered in Japan during 1956 as a result of improper disposal of methyl mercury, resulted in mercury poisoning (Timothy and Jane, 2001). In addition, spillage of waste water in Gold King Mine near Silverton had unexpectedly polluted the Animas River watershed. Successive flow of mine waste water from the tailings was further carried downstream by Animas River to the centre of Colorado, New Mexico and Utah. In turn, the river had turned into yellow by the action of oxidation and mobility of dissolved iron (Garrison and Times, 2017). In summary, these incidents highlight the adverse impacts towards environment, thus drawing the attention of worldwide to exploit effective solutions and measures in dealing with hazardous waste efficiently.

Implementation of waste management systems such as landfill, incineration and composting aim to treat massive amount of disposed wastes. Yet, removal of mobile and unstable heavy metals from these facilities are susceptible to enter the environment potentially by way of leaching process (Kasassi et al., 2017). Appendix A illustrates the overview pathways of waste streams, each route demonstrates proper waste management of heavy metals origin from its source to disposal site (US EPA, 2000).

In like manner, leaching process helps to ease the emission of heavy metals into nature, consequently contaminating the soil and groundwater. Owing to naturally mobility and non-biodegradable properties of heavy metals, they prone to accumulate at elevated level which threatened all forms of life. Selection of remediation technologies solely bases on the toxicity of heavy metals as well as the environmental parameters (US EPA, 2000). Nonetheless, exploitation of human in ferrous metal industries and agricultural applications have genuinely contributed the mass production of heavy metals significantly over years. By far, the most effective and efficient methods in elimination of heavy metal pollutions can be accomplished by solidification or stabilization technology (Anand, 2000).

Mobilization of heavy metals in ecosystem can be confined by utilizing S/S technique. Basically, it involves the encapsulation of heavy metals within the matrix. As a matter of fact, cement is commonly employed as a primary binder for S/S method, merit by its distinctive characteristics. Fixation of cement within S/S matrix enhances impermeable coating, ability to decrease hydraulic conductivity and constituent solubility as well as stimulating the reduction of contaminants (Roberts, 2001). In short, utilization of S/S matrix in leaching of heavy metals opens up promising applications in the future.

1.2 Mechanism of Leaching

The term "Leaching" is defined as a heterogeneous process in which organic solutes are being extracted from a carrier into a medium. Specifically, it involves extraction of organic solutes from solid matrix into leachate upon dissolving into a contacting liquid phase by means of percolation or dissolution. The dissolution rate of heavy metals into liquid phase may differ in response to the duration of contact period and other factors. For example, chemical, physical and biological factors are the primary parameters which account to solubility of heavy metals (US EPA, 2000). Likewise,

these dissolved constituents exhibit high degree of mobility in environment as they are capable of travelling downstream through porous medium or soil via diffusion and convection (Kasassi et al., 2017).

High permeability of heavy metals into leachate, which comprise of various composition and concentration of solutes have a possibility of affecting the quality of water. Moreover, infiltration of leachate from solid waste due to rapid growth of industrial development has predominantly interrupted the nature of environmental resources particularly in soil, underground and surface water. Instinctively, diffused pollutants are subsequently diluted by successive flow of surface water upon reaching it (US EPA, 2000). Chemical transformation of pollutants in soil as well as movability of pollutants into soil layers are crucial at the point of protecting groundwater from being contaminated by potential pollutants. In fact, it may take several years for a stagnant plume of pollutant to be flushed away from groundwater (Shrivastava and Mishra, 2011). In brief, risks related to run-off of heavy metals into the environment can be accessible by conducting several leaching test. For instance, leaching procedure such as toxicity characteristic (TCLP) and synthetic precipitation (SPLP) can be carried out. Performance of pancake column leaching test (PCLT) also helps to measure the probability of pollutants being emitted into the environment from a solidified mass (US EPA, 1992).

Migration of run-off leachates associated with heavy metals from unsaturated to saturated zone incurs contamination of groundwater. In reality, groundwater serves freshwater for industrial, domestic and livestock purposes, however contaminated groundwater consequently expose populations to heavy metals. Seeping of leachates rich in contaminants into groundwater significantly intrude the condition of soil and profusely remain in sediments before further release into surface water (US EPA, 2000). In conclusion, migration of contaminants from the surface water up to food chains at an elevated concentration, indeed, give rise to an overabundance of contaminants assimilated in body tissues, eventually harming the consumers (Volesky et al., 1983).

1.2.1   General Classifications of Leaching

At present, leaching procedures have been standardized in accordance with regulatory limits, serve to investigate upon the quantification of contaminants discharged into nature. Leaching of heavy metals stabilized in matrix complies with

several conditions inclusive of chemical, mechanical and geometrical properties of S/S matrix, rheological properties of leaching medium as well as experimental factors during leaching test (US EPA, 2001).

On account of complexity of mechanism, appropriate methods of leaching should be appointed to ease the experimental studies and researches, pertaining to seeping of heavy metals in dumpsite and landfill. After all, toxicity characteristics leaching procedure (TCLP) is an extraction method extensively employed in analyzing the degree of hazard inherent in wastes (US EPA, 1986). Experimentally, certain researchers claimed that TCLP has poor estimation in measuring concentration of arsenic, fluoride and selenium, yet over anticipate concentration of barium in leachate (US EPA, 2001). Intentionally, association of leaching procedures along with several tests serve to enhance precision in modelling the behaviour of heavy metals in nature (US EPA, 2003).

Standard operation of TCLP generally comprised of four primary phases. Principally, sample preparation is first established which involves particle size reduction, pH measurement and dilution of sample. Likewise, mode of contact with solid matrix in agitated system is defined during leaching stage. In addition, proper pre-treatment of leachate is performed by action of decantation, centrifugation or filtration primarily to define the properties of leachate for the purpose of instrumental analysis. Last but not least, leachate is analyzed under appropriate instrumental analysis so as to evaluate roles of each heavy metals present in leachate (Philip, 2004).

In a word, leaching can be basically categorized into two simple methods either by a static or dynamic method. In accordance to static methods, crushed block leaching test is further sorted into three different categories, consists of TCLP, SCLP and DWLP respectively. In fact, DWLP is formerly known as deionized water leaching procedure. Indeed, the performance of whole block leaching can be accomplished under monolithic leaching method. Additionally, serial batch, flow around and flow through leaching test are the three most common methods classified under dynamic method. By far, various types of leaching methods have been testified and implemented in compliance with specific heavy metals as attached in Table 1.1 (US EPA, 1986).

Table 1.1: Leaching Test Methodology

S. no.	Author/year	Method	Equipment	Metals
1	Shivpuri (2011)	(TLCP)	–	Fe, Zn, Mn, Ba
2	Palumbo (2009)	Column	Microtox 500 Analyzer	Al, As, Ba, Be, Bi, Cd, Co, Cr, Cs, Cu, Fi, Ga, Li, Ni, Pb, Rb, Se, Ag, Si, Ti, V, Zn
3	Sarade (2010)	Batch and TLCP	Atomic absorption spectrophotometer,	Zn, Ni, Cu, Fe, Pb, Mn, Mg, and Cd
4	Takao (2007)	Column	Diagenesis method	Ca, Na, Al, Si, B, Cr
5	Kazonich et al. (1999)	Column	–	Al, Ca, Fe, Mg, Mn, K, Na, Sb, As, Ba, Cr, Cu, Pb, Ni, Zn, Be
6	Sauer et al. (2011))	WLT & CLT	–	Cd, Cr, Se, and Ag,
7	Georgakopoulos (2002)	SGLP Leaching Leaching Column Test	ICP-MS using Elan 5000	Major (Si, Al, Fe, Ti, Ca, Mg, Na, K, and S) and trace (Ag, As, B, Ba, Be, Bi, Br etc)

Table 1.2: Leaching Criterions Endorsed by Malaysia

No.	Parameter	Unit	Standard Limit
1.	Temperature	˚C	40
2.	pH Value		6.0 – 9.0
3.	BOD_5 at 20 ˚C	mg/L	20
4.	COD	mg/L	400
5.	Suspended Solid	mg/L	50
6.	Ammoniacal Nitrogen	mg/L	5
7.	Mercury	mg/L	0.005
8.	Cadmium	mg/L	0.01
9.	Chromium, Hexavalent	mg/L	0.05
10.	Chromium, Trivalent	mg/L	0.20
11.	Arsenic	mg/L	0.05
12.	Cyanide	mg/L	0.05
13.	Lead	mg/L	0.10
14.	Copper	mg/L	0.20
15.	Manganese	mg/L	0.20
16.	Nickel	mg/L	0.20
17.	Tin	mg/L	0.20
18.	Zinc	mg/L	2.0
19.	Boron	mg/L	1.0
20.	Iron (Ferric)	mg/L	5.0
21.	Silver	mg/L	0.10
22.	Selenium	mg/L	0.02
23.	Barium	mg/L	1.0
24.	Fluoride	mg/L	2.0

1.2.2 Permissible Exposure Limits of Leachate

Municipal solid waste incinerator (MSWI) is a well-established technique that provides the option of treating residual wastes via appropriate combustion, resulting in volume reduction of residual wastes up to 80%. Typically, the incombustible ashes will then be further processed in waste landfill which comprised of multiple layers of polyethylene liners, thus diminish leachability of contaminants into nature. Performance of incineration coupled with landfilling promotes degradation of wastes efficiently, albeit vast capacity of valuable land is required (Sabbas and Polettini, 2003).

Conversely, run-off of wastes containing heavy metals from municipal landfill, consequently induces potential hazard towards the environment and population health. Hence, leaching regulatory limit is proposed to evaluate the tolerance of specific constituents for landfilling. In a word, regulatory leaching limits of heavy metals enforced by Ministry of Natural Resources and Environment, Malaysia are summarized in Table 1.2 (EQA Malaysia, 1974).

1.3 Problem Statement

Innovative processes for manufacturing large scale of production containing iron often incur severe contaminations towards the environment in view of inconsiderate disposal of waste products. For instance, illegal practice of dumping is primarily responsible for polluting both groundwater and soil. Alternatively, run-off of iron residue from municipal solid waste incinerator (MSWI) as bottom ash is classified as one of the major causes of contamination. Likewise, continuously discharging of electroplating sludge and iron blue pigments particularly into the ocean are regarded as the primary anthropogenic emission of iron sources, eventually exert significant risks to living organisms (Kasassi et al., 2017). High extend of mobility and stability inherent in iron give rise to its persistent in the natural environment as it is not readily to be degradable nor decayed, consequently bio-accumulate in living tissues at an elevated amount (US EPA, 2000). At present, S/S is considered to be the most promising technology for leachability control as compared to numerous established techniques, which aims to restrict the mobility of iron ions from exposing into the nature. The main objective in utilization of S/S is to diminish the bioavailability of heavy metals in ecosystem via encapsulation within an inert matrix (Anand, 2000).

In fact, incorporation of pozzolan materials into Ordinary Portland Cement (OPC) results in the formation of stable calcium silicates, predominantly introduced to strengthen the structure of C-S-H gel yet exhibits fundamental cementitious properties. The formation of calcium silicate hydrate via hydration of OPC aid to enhance the efficiency in diminishing leachability of heavy metals (Sata, 2007). Nevertheless, rice husk ash (RHA) which embodied with 95% of silica content can be utilized as an alternative to supplant sand as it is economically available in Malaysia (Naji, 2010). In summary, the principal part of this research is to justify the effectiveness in treating leachability of heavy metals via utilizing OPC as settling agent coupled with RHA as a pozzolanic additive.

1.4   Aim and Objectives

The primary focus of this research project is to investigate the relationship between the leachability of Iron in cement cube in accordance with the effect of RHA as a pozzolanic additive. In essence, well-defined objectives are established as below aim to achieve the desired goal.

1. To appraise leachability of Iron and Calcium from samples via Plasma Optical Emission Spectrometry (ICP-OES).

2. To evaluate changes of pH over contact period.

3. To justify the presence of compounds in cement matrix by way of X-ray diffractometer (XRD).

4. To interpret microstructure of cement matrix through scanning electron microscopy (SEM).

5. To identify elemental compositions inherent in cement cube via energy dispersive X-ray spectroscopy (EDX).

CHAPTER 2

LITERATURE REVIEW

2.1   Toxicology of Heavy Metals in the Indigenous Habitat

Scientifically, the phrase "Heavy Metal" is defined as a metallic element which is not metabolically degradable and its accumulation in living tissues may result in death and critical health threats. Consequently, heavy metals that exhibit the specific gravity of more than 5 possess tendency in causing disastrous effects to living organisms even at a low level of concentration (Garbarino et al., 1995). By nature, acidic rain breaks down soils and eventually discharging heavy metals into rivers, lakes, groundwater and streams. Breakdown of inert-pair bonding between heavy metals and rocks due to weathering of soil further releasing heavy metals into the environment as well as the atmosphere in notable concentration. Conversely, exploitation of mineral resources at extreme rates create elevated local level of metals which capable of migrating to the immediate environment, hence toxicity characterization of heavy metals need to be performed beforehand prior to proper waste disposal as shown in Appendix B (US EPA, 2000).

Moreover, dispersion of toxic pollutants as a result of man-made sources prone to persist in the environment as dispersed pollutants are not readily to be recovered nor reassembled, hence resulting in everlasting environmental issues. Radioactive isotopes have been discovered and opened up a new route in breaking down of heavy metals via radiation (Chaychian et al., 1998).

Toxicity of heavy metals may varied in respect to other factors. Allocation of metallic elements through ingestion from contaminated sources eases the assimilation of metals in living tissues, resulting in failure of cellular functions as well as long-term disabilities in human. Nevertheless, bioaccumulation of heavy metals in organisms prone to get concentrated quicker than excretion. In fact, experimental studies have shown that $10^5 - 10^7$ of metal enrichment coefficient can be deposited in cells (Volesky et al., 1983).

In the aquatic system, destructive power of heavy metals can incur sub-lethal effects, remarkably in hindering growth and reproduction of aquatic invertebrate. Biologically, absorption of heavy metals as free ions upon direct uptake, correspondingly disrupts the cellular metabolism of aquatic life (El-Moselhy et al.,

2014). Terrestrial invertebrates and plants are fairly tolerant to metallic elements as they do not exhibit any hostile affect (Tangahu et al., 2011).

In contrast, consumption trace amount of metallic elements plays an important role in maintaining the metabolism of living organisms. Clinically proven that consumption right amount of metals is healthy for daily life. In an ironic manner, an elevated level of exposure constituted by metallic elements adversely incite detrimental effects and health hazards as shown in Table 2.1 (US EPA, 1993).

Table 2.1: Toxicology of Heavy Metals

| Metal Contaminant | Permissible limits by International bodies (mg/L) | | Health Hazard |
	WHO limit Drinking Water (2010)	US EPA (1993)	
Arsenic	0.01	5	Carcinogenic effect, initiator of liver and skin tumours, gastrointestinal effect
Mercury	0.001	0.2	Corrosive to sensory organs and muscle membrane, initiator of dermatitis and anorexia, potential of kidney failure
Cadmium	0.003	1	Carcinogenic effect, incur lung fibrosis, weight loss potential
Lead	0.01	5	Carcinogen potential, loss of appetite and diminish IQ, initiator of anaemia and sterility, incur kidney failure and elevated blood pressure
Chromium	0.005	5	Carcinogen potential, initiator of lung tumours, incur allergic dermatitis
Nickel	0.02	-	Chronic bronchitis, incur lung failure, initiator of nasal sinus
Zinc	3	-	Incite short term illness, namely "metal fume fever"
Copper	2	-	Irritation to sensory organs, chronic headache and stomach-ache, incur severe dizziness, initiator of diarrhoea

2.2 Sources of Iron in Nature

Iron is one of the metallic element lies in group 8 of the periodic table. It exhibits the characteristics of typical transition elements by forming variable oxidation states and coloured compounds. By nature, ferrous iron and ferric iron are the most common range of oxidative states existed on the surface of earth. Physically, both ferrous and ferric ions will produce different colours upon dissolving in solutions respectively. For instance, a violet colour solution is observed when ferrous ions dissolved whereas ferric ions formed yellow brown solution (Bolm, 2009).

In recent years, industrial application of iron has been increasing exponentially, owing to high demands of market needs. At present, the potential of human exposure and water sources towards iron have increased dramatically as a result of an increase in operation. For instance, spillage of iron into the environment has greatly polluted and affected the quality of water in dams, water reservoir as well as underground water wells (Siemiatycki et al., 2004). Generally, environmental issues and challenges always subjected to public awareness and financial interests. In the long run, by performing an appropriate level of leaching that considered safe to public health and environment might help to reduce certain uncertainties and constraints encountered.

2.2.1 Commercial Application of Iron

Iron is the fourth common element available in the earth crust (Frey and Reed, 2012). Owing to its relatively low cost and a high degree of ductility, iron is widely used in engineering applications such as building constructions, fabrication of body panels for automobiles as well as the construction of machinery tools. Moreover, iron also plays an essential role as catalyst for commercial production such as Haber-Bosch and Fischer-Tropsch Process (Kolasinski, 2002).

Commercially available iron usually deployed in metallurgical process, accounting for production of refined metals such as cast irons, wrought irons and various type of alloys. In metallurgy, stainless steel is tailored by combination of iron with varying amount of chemical elements such as chromium, manganese, silicon, nickel, molybdenum and trace amount of nitrogen. Chromium is entitled to "Guardian of Metal". This is because an addition 10% of chromium into alloys exhibits the formation of a thin layer of Cr_2O_3 which helps to prevent the formation of rust and unwanted stain on the surface. Additionally, presence of alloying

elements enhance the chemical properties of stainless steel by exhibiting high resistance towards high temperature and pressure (James and Stephen, 2004).

In recent years, superior properties of iron in term of heat resistance and chemically inert have overtaken lead and dominated in the field of radiation protection. It is proven that iron is much more reliable and stronger mechanically than other shielding materials in attenuating photons and neutrons despite of its low weight (Berndt et al., 2010).

Foremost, iron is basically one of the key components used in application of paints, dyes, pigments and colour of various geological formations. Its pigments capable of contributing yellowish colour for sculpture and historical buildings (Dickinson and Robert, 1964). Moreover, iron is also deployed widely in manufacturing of ink. Mixture of tannin and iron salts enhance the solubility by forming a water soluble ferrous tannate complex which eases the rate of penetration and achieves permanent stain colour (Gutenberg, 2013). Commercially, rapid growth on the development of iron is often essential in modern industry for achieving improved properties of ferroalloys.

2.3   Exposure Pathway and Adverse Effects of Iron

Daily iron exposure route can be classified into three primary pathways. These pathways basically involve dermal contact and ingestion whereas inhalation of iron primarily contributed by occupational exposure (OSHA, 2014). Notwithstanding that trace amounts of iron uptake does not pose a critical threat, however excessive iron consumption and exposure to high level of iron contamination particularly in sea or ocean will contribute significant impacts directly towards both aquatic life and public health.

2.3.1   Effect of Iron on Health

As a matter of fact, ferrous iron is proven to have high toxicity as compared to ferric iron by causing severe effects ranging from mild irritation to cancerous condition due to its high absorption rate (Papanikolaou, 2005). Consumption of drinking water from iron pipes via oral ingestion, leading causes of iron poisoning. Biologically, iron preferably forms numbers of harmful free radicals which capable of initiating lipid peroxidation and depolymerizing DNA strands (Grazuleviciene, 2009). Besides, ingestion of iron above 0.05 grams able to induce fatal within 24 hours regardless of

children or adults in view of liver failure as tabulated in Table 2.2 (Tokar et al., 2013). Nonetheless, eyes come in contact with iron particles result in siderosis. Susceptibility to allergic responds for instance asthma and dermatitis in response to dermal contact of both ferrous and ferric compounds (Yoshihisa and Shimizu, 2012). Occupational exposure to iron by way of chronic inhalation eventually leads to a risk of lung cancer. In addition, ferrous and ferric ions also show potential in promoting mutagenic and genotoxic effects (Toyokuni, 2002). As a result, iron is classified as probable carcinogenic substance in accordance with epidemiological and experimental studies (Siemiatycki et al., 2004).

Table 2.2: Tolerable Upper Intake Level

Group Age		Tolerable Upper Intake Level			
		Selenium	Iron	Copper	Zinc
Children	1–3 yr	90 μg	40 mg	1000 μg	7 mg
	4–8 yr	150 μg	40 mg	3000 μg	12 mg
Males	9–18 yr	300 μg	40–45 mg	7000 μg	34 mg
	19–70 yr	400 μg	45 mg	10000 μg	40 mg
Females	9–18 yr	300 μg	40–45 mg	7000 μg	34 mg
	19–70 yr	400 μg	45 mg	10000 μg	40 mg

2.3.2 Effect of Iron on Environment

In like manner, dispersed iron adversely affect all living organisms in the environment, specifically the soluble ferrous form. Presence of ferrous and ferric iron in the environment as a result of unprecedented human activities. In fact, ferrous iron tends to form insoluble ferric iron in presence of high oxygen concentration. Suspension of ferric iron is fairly stable in water and capable of travelling further downstream. Exposure of 0.1 to 20 mg of iron per litre of medium (USGS Groundwater Monitoring Data) is adequate to cause a lethal effect on aquatic life. High concentration of iron accumulates in fish tissue eventually damages the respiratory system and suppresses respiration (Teien et al., 2008). Likewise, concentration of iron below 0.01mg per litre is sufficient to alter the reproduction of Daphnia (Zhang et al., 2016).

On the other hand, plants do not exhibit any acute iron toxicity, it is reckoned that primary iron intoxication in plants is predominantly due to iron deficiency which resulting in chlorosis (Connolly and Guerinot, 2002). For instance, most plants exhibit toxic effects once exposed to feed concentrations of iron between 5 to 200ppm. Generally, an adequate amount of iron present in soil is vital for photosynthesis and growth rate of plants. Hence, uptake of iron is achievable by either reduction or chelation-based mechanism (Kim and Guerinot, 2017). In general, safety handling and disposal of iron need to be taken into consideration, albeit to varying distinct properties between ferrous and ferric iron.

2.4 Fundamentals of Iron Chemistry

At present, the most common forms of iron existed in the environment are oxides and ions as a result of its significant redox potential. Instinctively, these compounds exhibit the fundamental properties of free elements as compared to metallic iron in nature. For instance, surface of iron comes in contact with oxygen in the atmosphere, subsequently resulting in a formation of intensely coloured iron oxide. Likewise, iron reacts aggressively to form complex ions upon dissolving in a medium by nature of ligands (Kosaka et al., 2015). Typically, a pale green colour of ferrous ions turns into violet colour when dissolved in water. The same goes to ferric ions which appeared blood-red colour upon mixing with thiocyanate ions (Cotton and Wilkinson, 1988).

2.4.1 Redox Mechanism

For simplicity, oxidation-reduction reaction is formerly known as Redox Reaction which involves the transferring of electrons between two species. Redox reaction exhibits the ability to undergo both oxidation and reduction simultaneously by changing the oxidative number of molecules via gaining or losing an electron (Libre Texts, 2013). Merit by redox properties of iron, a brilliantly red complexes which obtained by combining ferric and thiocyanate ions together are incurred by the presence of SCN^- and $FeSCN^{+2}$. Iron (II) thiocyanate is commonly used to verify the presence of peroxides by oxidizing pale green $Fe(SCN)_2 \cdot 3\,H_2O$ crystal to a bright red solution as shown in equation 2.1 and 2.2 (Lewin and Wagner, 1953).

$$Fe^{3+} + SCN^- \rightarrow [FeSCN]^{2+} \tag{2.1}$$

$$[Fe(H_2O)_6]^{3+} + SCN^- \rightarrow [Fe(H_2O)_5]^{2+} + H_2O \tag{2.2}$$
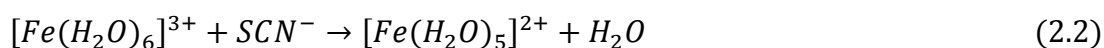
Nevertheless, both ferrous and ferric ions have the ability to form stable complexes with cyanide ions. Alternatively, a combination of these ions under different oxidation state contributes an intensely Prussian blue coloured pigment as shown in equation 2.3 and 2.4. The same coloured expression is likely to be achievable via reaction of $Fe(CN)_6{}^{3+}$ and ferrous ions (Cotton and Wilkinson, 1988).

$$K_4Fe(CN)_6 + Fe^{3+} \rightarrow KFe[(CN)_6] + 3\,K^+ \tag{2.3}$$

$$K_3Fe(CN)_6 + Fe^{2+} \rightarrow KFe[(CN)_6] + 2\,K^+ \tag{2.4}$$
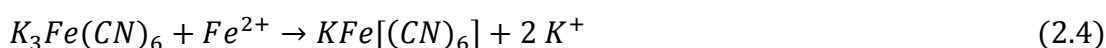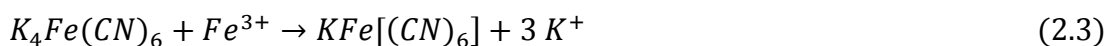
Foremost, iron is best known for its redox reaction with oxygen in presence of moisture, resulting in the formation of rust. Iron mass will entirely disintegrate given that sufficient time and oxidizing agents are provided. Subsequently, both $Fe(OH)_2$ and $Fe(OH)_3$ will dissociate partially to form FeO and $FeO(OH)$ due to dehydration equilibrium while $FeO(OH)$ will further dissociate, forming Fe_2O_3 as expressed in equation 2.5 and 2.6. As a result, a thin layer of stable iron oxide is formed, resulting in red hydrated Fe_2O_3 to be deposited. Fe_2O_3 is regarded as the principal element of red-brown rust in solution as shown in equation 2.7 (Gräfen et al., 2000).

$$Fe(OH)_2 \leftrightarrow FeO + H_2O \tag{2.5}$$

$$Fe(OH)_3 \leftrightarrow FeO(OH) + H_2O \tag{2.6}$$

$$2\,FeO(OH) \leftrightarrow Fe_2O_3 + H_2O \tag{2.7}$$

Physiological role of iron ions in living organisms are essential in the transportation of oxygen, a mechanism which binds oxygen with haemoglobin to enable proper oxygenation (Jensen and Ryde, 2004). Moreover, naturally occurring iron exhibits four stable isotopes, consists of Fe^{54}, Fe^{56}, Fe^{57} and Fe^{58} (Anbar, 2004). In term of magnetism, ferrous ion exhibits dimagnetic properties coupled with the formation of low-spin complexes. On the other hand, ferric ion only exhibits paramagnetic properties due to its availability of single lone electron (Istomin Duchkov, 2008). In recent years, anthropogenic activities adversely disrupt the iron cycle particularly in the ocean as shown in Figure 2.1, subsequently promoting significant risk to the ecosystem (US EPA, 2001). Hence, various treatment technologies and techniques have been developed to serve remediation purposes.
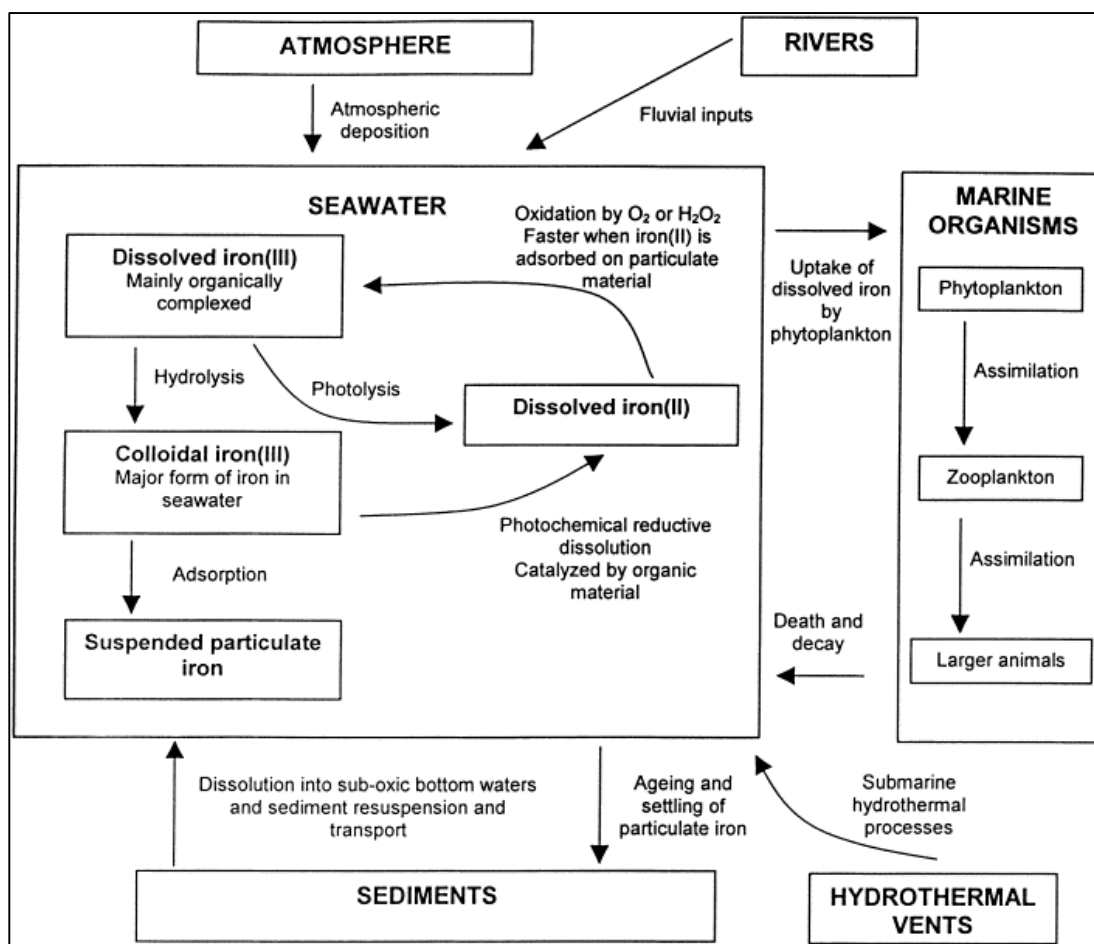
Figure 2.1: Illustration of Iron Cycle

2.5 Ordinary Portland Cement (OPC)

Commercially available cement typically produced from $CaCO_3$ in mass production, combusted in a controlled-manner. Ultimately, calcium hydroxide is the final output of lime stone upon consumption of water. Incorporation of clay during the process of cement, prior to generation of anhydrous aluminosilicate. Mortar-structured of calcium silicate gel (C-S-H) which is specially formulated via hydration of calcium hydroxide with aluminosilicate, exhibits robust mechanical properties as shown in equation 2.8 (Sata, 2007).

$$Al_2Si_2O_7 + Ca(OH)_2 + H_2O \rightarrow C - S - H \tag{2.8}$$
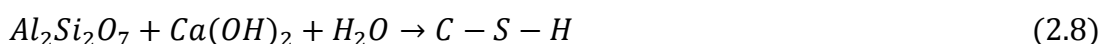
On the contrary, solidified matrix allocates attainable porous region which eases the leaching of metal ions. Nonetheless, the porosity of solidified matrix can be resolved merit to distinctive properties inherent in C-S-H, subsequently filling the

adjacent pores. In summary, leachability of ions is appreciably disrupted due to low hydraulic conductivity, thus capable to impede leaching of metal ions (Sata, 2007).

2.5.1 Hydration of Cement

Commercially available Portland cement is rich in dicalcium (C_2S) and tricalcium silicate (C_3S) respectively. Moreover, both tricalcium aluminate (C_3A) and tetracalcium aluminoferrite (C_4AF) are obtainable from cement in vast quantities. Gypsum is also reckoned as the major component which embedded profusely in Portland cement. Chemical reactions exhibited by respective compounds are likely to be initiated via series of hydration. The overall weight percent of constituents complied with Cement Chemist Notation are tabulated in Table 2.3 (Chen, 2004).

Table 2.3: Mineralogy of Cement

Constituent	Pozzolana	OPC
SiO_2	62.03	19.7
Al_2O_3	16.66	5
Fe_2O_3	12.98	3.16
CaO	0.21	63.03
MgO	1.75	1.75
SO_3	0.16	2.8
LOI	2.97	2.58
Insoluble Residue	47.24	2.98
Mineralogy		
C_3S		61
C_2S		11
C_3A		8
C_4AF		10

Ettringite is the output subjected to an incorporation of gypsum and tricalcium aluminate merit to hydration as expressed in equation 2.9. Tricalcium aluminate reacts promptly with water to produce calcium silicate hydrates as well as lime. Likewise, ettringite is further decomposed into hydrate crystal containing monosulfate aluminate as shown in equation 2.10. Conversion of calcium silicate hydrate from dicalcium and tricalcium silicate are achievable via the addition of water. In fact, conversion of ettringite is relative to the proportion of (CSH_2) and (C_3A) present in the early stage. Production of ettringite is favourable with respect to

the high availability of tricalcium aluminate, hence elongated needle-like structured of ettringite is observed (Thomas et al., 2003).

Ettringite:

$$[AlO_4]^- + 3\,[SO_4]^{2-} + 6\,[Ca]^{2+} + aq. \rightarrow C_6AS_3H_{32} \tag{2.9}$$

Monosulphate:

$$[AlO_4]^- + [SO_4]^{2-} + 4\,[Ca]^{2+} + aq. \rightarrow C_4ASH_{18} \tag{2.10}$$
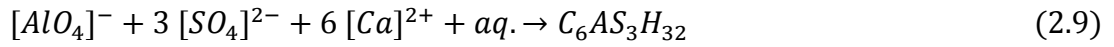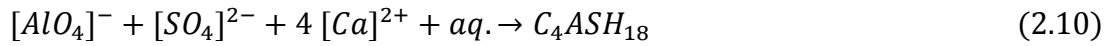
Both calcium silicate hydrogel and calcium hydroxide arise copiously owing to series of hydration, sufficiently retaining the structure of cement particles in term of the cohesive block via formation of persistence layer as expressed in equation 2.11, 2.12 and 2.13. In the midst of curing, an evolution of silica gel is initiated which eventually subsiding in an attainable porous region. Foremost, proper structured C-S-H gel perpetually denoted by specific Ca/Si ratio which varied from 1.8 to 2. Distinctly, certain hydration products fail to promote durability properties relative to poor bonding with contact-phase, albeit to intrinsically sturdy properties inherent in respective hydration products (Chen, 2004).

$$2\,C_3S + 6\,H \rightarrow C_3S_2H_3 + 3\,H \tag{2.11}$$
$$2\,C_2S + 4\,H \rightarrow C_3S_2H_3 + CH \tag{2.12}$$
$$C_3A + 6\,H \rightarrow C_3AH_6 \tag{2.13}$$

2.6 Rice Husk Ash (RHA)

Auxiliary slag containing silica is applicable to reduce the availability of surplus calcium hydroxide, liable to the evolvement of C-S-H gel. Coherently, naturally occurring pozzolans which arise originally from fly ash and rice husk ash (RHA) are termed as water insoluble silicate merit to the existence of oxyanionic silicon($SiO_3{}^{2-}$). Incorporation of lime coupled with Portland cement as setting agent aid to initiate the cementitious properties of individual materials, chiefly contributing in endurance development (Stanley, 2008).

2.6.1 Pozzolanic Reaction

Enhancement of rice husk ash (RHA) can be achievable via combustion in a controlled manner, aim to yield desirable distinctive properties of RHA in term of porosity, overall external surface area as well as weight characteristic. Commercially, RHA is listed as the most prominent additive available in the market merit to the vast quantities of silica inherent in the ashes, likewise economically feasible. Morphology of silica embodied in RHA perpetually subjected to various operating conditions such as temperature, pressure as well as duration. Essentially, highly reactive amorphous silica is harvested relative to appropriate combustion, generally operated at the temperature ranging from 500˚C to 700˚C which extended up to 12 hours. Elevated content of carbon is likely to be obtained, pertaining to the exposure of short heating duration. In summary, naturally occurring silica embodied in RHA prone to exhibit fundamentals cementitious properties upon reacting with OPC (Stanley, 2008).

2.7 Principles of Remediation Technology

Substantial concentration of iron in the environment necessitates treatment technologies be invested, as to devise reliable remediation processes in order to regulate iron contaminations. Principally, toxicity reduction methods are accessed based on the approach of toxicity tracking as well as toxicity identification evaluation. Moreover, destruction and removal treatments in term of chemical precipitation, ion-exchange and application of membrane filtration are the most conventional approaches.

At present, containment technologies specifically utilization of S/S are regarded as the most effective approaches in remediating contaminations issued by iron. Ingenuity in optimization and application of engineering knowledge in the field of remediation design, site conditions as well as strong inclination in biogeochemical properties inherent in both soil matrix and iron are essential in resolving appraisal of treatments as illustrated in Figure 2.2 (US EPA, 2001).

```
┌─────────────────────────────────────────────────────────────────────────────────────────┐
│              Remedial Options for Metal-Contaminated Soils (US EPA, 2001)                 │
└─────────────────────────────────────────────────────────────────────────────────────────┘
```

	Extraction of metals		REMEDIATION STRATEGY	Immobilization/isolation of metals	
	Ex situ	In situ	REMEDIATION LOCATION	Ex situ	In situ
	Soil Washing Physical separation Chemical extraction Biological extraction Eletrokinetic	Electrokinetics Phytoextraction Soil flushing	TREATMENT TECHNOLOGIES	Stabilization/ solidification	Stabilization/ solidification Phytostabilization Biological Stabilization
			CONTAINMENT/ DISPOSAL TECHNOLOGIES	Off-site disposal (or off-site landfilling)	In situ containment (capping and barrier)

Figure 2.2: Remediation Technology

2.7.1 Conventional Removal Approaches

Assessment of toxicity inherent in contaminants is accomplished via toxicity reduction procedure, aims to distinguish undesired output by experiencing reduction. Destruction method is impracticable owing to high consumption of energy, economically infeasible. Chemical precipitation is performed merit to its simplicity, liable to produce insoluble sediments via hydrogen or sulfide precipitation. Instinctively, removal of iron from the water source is accessible by ion-exchange coupled with granular activated carbon. Performance of reverse osmosis via membrane filtration proves to evacuate substantial iron ions with high effectiveness despite of its extended expenses as well as process complexity. Extraction of iron from soil is achievable via soil venting. Nevertheless, ex-situ treatment is likely to be established in response to eradication of iron originated from contaminated groundwater (Fu and Wang, 2011).

2.7.2 Fundamentals of Containment Methodology

Possibility of hazardous constituents from disseminating into the environment will be likely to diminish via assorted containment practices inclusive of bio-stabilization, encapsulation and S/S techniques. In contrast, zero accomplishment is achieved relative to the run-off of iron from containment zone in view of passivation layer deposited onto the permeable reactive barrier, chiefly resulting in weak isolation properties (US EPA, 2000). Principally, S/S technology promotes encapsulation of ions via involvement of inert matrix, serves as an attainable region for attachment of ions. Merit to extensive fixation of iron (III) compounds relative to cement as an inert matrix, enabling to confine mobility of ions from dispersing freely into a wide region. Nevertheless, S/S technique is effective in dealing shallow site within a particular depth, ranging from 2 to 5 meters (Anand, 2000). Leachability of iron via regular cement is significant in comparison with slag-modified cement on account of low slag content, sufficiently reliable to the high degree of leaching (US EPA, 2000). Moreover, loss on ignition (LOI) is introduced upon combustion at a specified temperature, intent to justify the existence of carbon content available in Portland cement. In brief, such leachability necessitates much preliminary studies be conducted to activate mechanism of S/S. Table 2.4 expressed the advantages and limitations inherent in respective remediation approaches.

Table 2.4: Characterization of Available Remediation Techniques

Technology	Description	Advantages	Disadvantages
Stabilization/ Solidification (S/S)	S/S employed widely in cement process, intended to immobilize and entrap metals in a modified soil matrix	S/S is favourable to extensive range of contaminants and soil species	Volume of treated sample likely to be increased via S/S method
In-situ chemical stabilization	Reduction of metal bioavailability and solubility without incur impact towards soil matrix	Applicable for site vegetation in a large scale	Hazardous and non-cost effective chemical agent is required
Phytoremediation	Utilization of plants as to avoid soil erosion due to wind and rain, liable to migration of metals to groundwater	Applicable for broad range of metals, limited area of treatment, low disposal rate of contaminated biomass	Liability matters in term of maintenance, controlling of site, limited to certain depth of root zone
Electro kinetics	Removal of saturated metals from soil via electrochemical approach. In-situ method is favoured than ex-situ	Effectiveness in removal of metals from soil by in-situ method, suitable for various type of metals	Allowable limit for saturated and partial saturated soil, availability of multi metals leads to site contamination
Biological Extraction	Utilization of microbial activity to diminish metals toxicity, coupled with chemical stabilization	Potential loss of biological receptors in human. Contribution to site vegetation	Pilot studies are required to treat efficiency, liability matters and indefinite maintenance

2.8 Variability of Parameters towards Leachability of Iron

Extend of mobility inherent in heavy metals may differ relative to the degree of alkalinity and acidity of leachate. Mobility of heavy metals is enhanced merit to the increment of hydrogen ions present in acidic leachate. Vice versa, alkaline leachate exhibits elevated concentration of hydroxide ions, authentically induce the decrement of mobility displayed by heavy metals. Thus, pH serves as an essential measurement prior to the justification of mobility behaved by respective heavy metals. In short, researchers strive to relate leachability of iron with respect to pH, albeit to varying parameters involved (Kasassi et al., 2017).

2.8.1 Leachate pH as Function of Time

Behavioral variances of iron with respect to time contemplated by J.D. Hem and W.H. Cropper via taking advantage of Plexiglas columns, prior to evaluation of landfill leachate subjected to pH change (Hem and Cropper, 1959).

On account of the performance of S/S in term of adjusted phase and transitional phase is cursory in the landfill, hence alteration of pH in leachate is perceptible preceding to the early stage of test conducted for entire samples. Organic acids emerged from microbial activities where responsible for the decrement of pH level in leachate. Dissolution of heavy metals measured up to a considerable extent, steadily imposed by excessively low pH scale. Moreover, a miscellaneous ambience of landfills such as anaerobic environment, chiefly initiates rapid acidification as well as methanogenic phase. Ultimately, the landfill is likely to be characterized as a mature stage in which pH essentially falls within 6 to 8 (Frey and Reed, 2012).

ICP-OES analysis infers that leaching concentration of iron customarily starts off with a moderate decrement, right off mounting incrementally. First peak of leaching concentration is possibly to be developed within 10 days. Second peak is achievable upon reaching 40 days, whereas minimum peak is observable right up to 50 days of experiment (Hem and Cropper, 1959). On the whole, naturally occurring iron prone to exhibit a high degree of leaching in an acidic environment.

2.8.2 Relationship of Ferrous-Ferric System and Redox Potential (Eh)

Naturally occurring ferric hydroxide, $Fe(OH)_3$ is predominantly expressed as a solid phase on account of its poor solubility at equilibrium pH within 5 to 8. Moreover, ferrite (FeO_2^-) is likely to arise due to the availability of alkalinity condition. Elevated concentration of FeO_4^{2-} is perceptible merit to distinctive redox reaction. Conversely, ferrous hydroxide $Fe(OH)_2$ exhibits a high degree of basicity as compared to ferric hydroxide. Both Fe^{2+} and $FeOH^+$ are the fundamental outputs via ionization. Complex anions such as hypoferrite (FeO_2^{2-}) generally occurred in alkaline medium. Fluoride and chloride complexes commonly contribute pH values that fairly fall below the region of bicarbonate carbon dioxide. Figure 2.3 illustrates the speciation and solubility of ferrous-ferric system in solution by Visual MINTEQ model (Hem and Cropper, 1959).
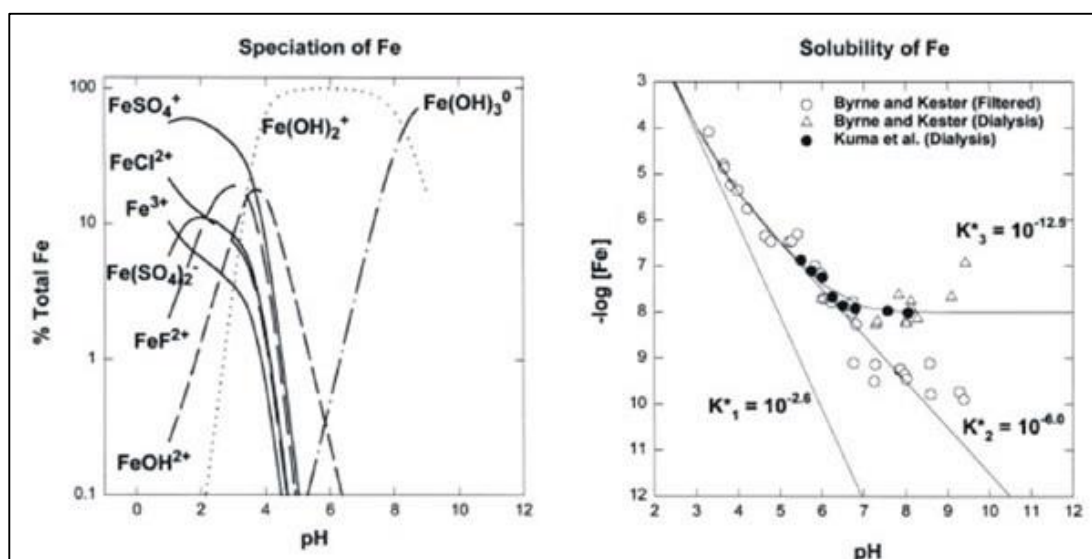
Figure 2.3: Speciation and Solubility Diagram of Ferrous-Ferric System

Nernst equation is introduced as to investigate the relationship lies between oxidized and reduced species via quantitative expressions. In fact, performance of ferrous and ferric ions merely depend on the pH inherent in solution as well as subjected to the precipitation of hydroxide complexes.

In effect, researchers strive to estimate species of iron ions involved in leachate, thus an overview of Eh-pH diagram for ferrous-ferric system is illustrated in Figure 2.4. Advanced discussions remain committed to study the distribution of iron species in term of precipitated, dissolved and sorbed phases. Dissolved

constituents often interpreted as dominant species, responsible in quantifying toxicity of iron inherent in leachate. In a word, substantial exposure of iron towards environment necessitates remediation technologies to be devised prior to manipulate the threshold limit of contaminants (Hem and Cropper, 1959).
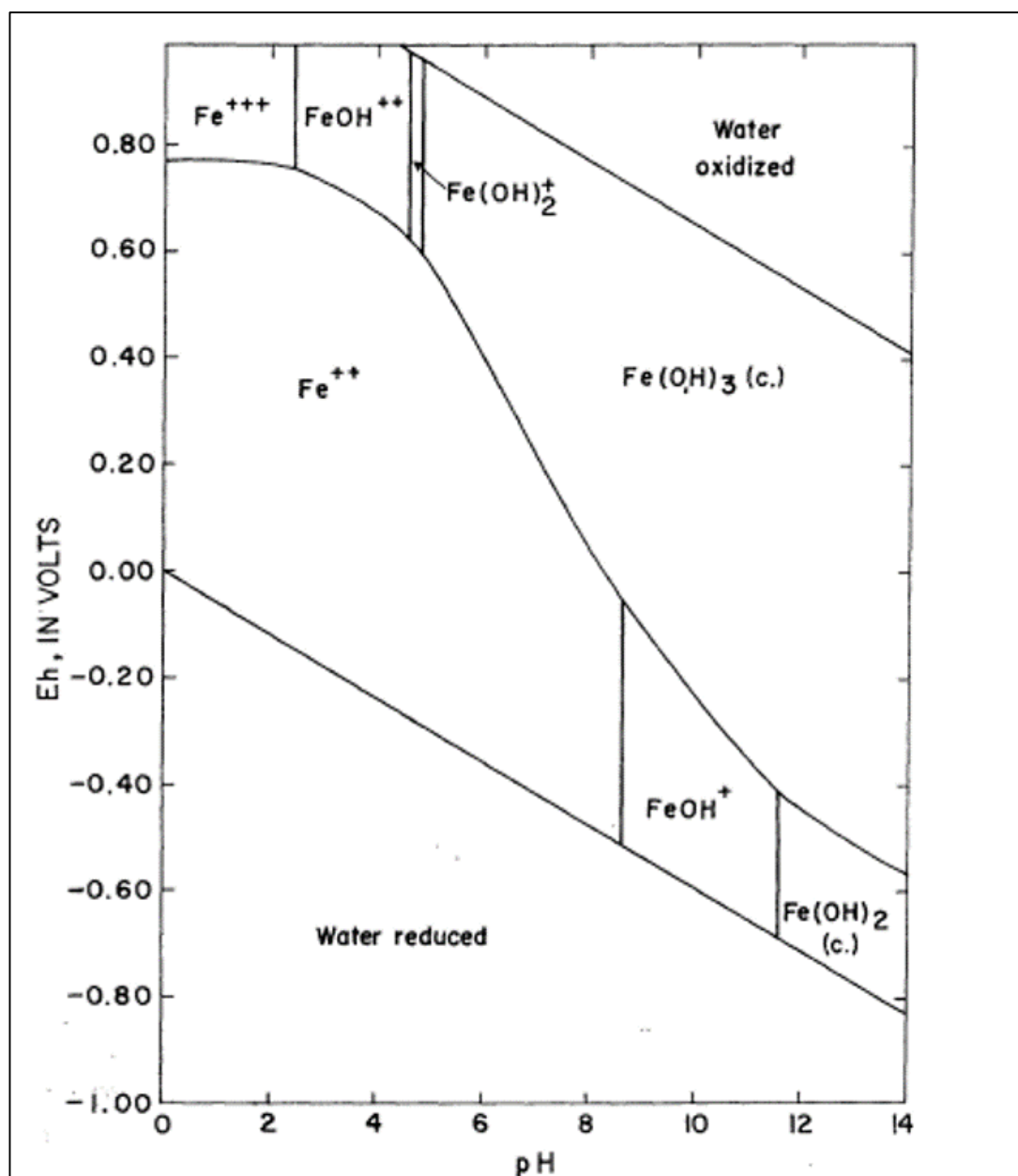
Figure 2.4: Eh-pH Diagram of Ferrous-Ferric System

CHAPTER 3

METHODOLOGY

3.1 Research Methodology

Leachability of iron was analyzed by means of whole block leaching procedure, formerly known as monolithic leaching method. Prepared blocks were perfectly shaped into customized geometric cubes, aid to sustain its structure throughout experiment. These shaped blocks were then transferred to a 60 ml diluted acetic acid solution which set at a pH of 2.88. The measured pH 2.88 of acetic acid was a standard enforced by US EPA as to evaluate the disposability of wastes in the landfill (Roger and Caijun, 2004). Buffer solutions labelled with pH of 2.88 and 4.93 were established by US EPA 311 method which intended to appraise landfill condition. Basic properties exhibited by cement block merit by its existence of metal hydroxide and oxide, hence pH 2.88 was utilized. Instrumental results were justified by an action of triplicate mode to verify reproducibility and reliability (ALS Environment, 2000).

3.1.1 Preparation of Cement Blocks

Initially, Ordinary Portland Cement (OPC) was compacted into desired geometry with the aid of cupboard mould that had been customized into cuboid with a dimension of 25mm x 25mm x 25mm. Acetic acid composed of pH 2.88 ± 0.5 was measured up to a volume of 60ml, aimed to facilitate the suspension of cubes in solution (US EPA, 1986).

Several variables were manipulated. Each experiment set was immersed in a beaker containing acetic acid, associated with 9 distinct durations which extended to 28 days. Contact time varied respectively from 1, 4, 7 and 14 hours, additionally 1, 4, 7, 14, 28 days were subjected as to treat leachability of iron. Compacted cement blocks coupled with respective iron concentration which constituted of 0 ppm, 10k ppm, 30k ppm were conducted for each stipulated duration. Iron concentration of 0 ppm was treated as a criterion of control group. Adequate measure of combusted RHA was prepared and added into the cement, acts as an additional binder. 5 wt% of RHA which doped into OPC was introduced for each respective samples of 10k ppm, 30k ppm, inclusive of standard control group 0 ppm prior to casting and leaching

purposes (US EPA, 1986). In like manner, 6 sets of trial test which differed from composition were conducted, extended to 9 durations via triplicate, resulted in 162 of cubes to be cast. The comprehensive specifications of cement cube samples carried out in this experimental study are labelled in Table 3.1

Table 3.1: Specification of Cement Cube Samples

Sample	Water Mixture	Binder Mixture		w/b ratio
	Fe 3+ Solution (g)	Cement (g)	RHA (g)	
100 OPC	-	1500	0	0.33
100 OPC + 10k Fe	500	1500	0	0.33
100 OPC + 30k Fe	500	1500	0	0.33
95 OPC + 5 RHA	-	1425	75	0.33
95 OPC + 5 RHA + 10k Fe	500	1425	75	0.33
95 OPC + 5 RHA + 30k Fe	500	1425	75	0.33

Note: 100 OPC + 10k Fe denoted as 100 % OPC mixed with 10,000 ppm Fe

: 95 OPC + 5 RHA denoted as 95 % OPC incorporated with 5 % RHA

Mixture of solvent and solidified samples in the experiment, namely leachate and cubes. Leachate was transferred to ICP-OES for quantitative determination, likewise characterization of pH via pH meter. A randomly chosen block was pounded into a thin section, ease the study of surface morphology conducted by SEM analysis. In addition, EDX was introduced to clarify elemental composition. Compositional determination of the remaining powdered samples was inspected via performance of XRD analysis.

3.1.2   Preparation of Iron Nitrate Solution

Chemicals used throughout the experiment were purchased from a company named Synertec Enterprise. Naturally occurring iron may present in various form depending on the surrounding conditions, commonly exist in the form of oxide and hydroxide. Correspondingly, iron (III) nitrate nanohydrate was preferred as the source of iron (III) ions merit by its high degree of dissociation in cement as well as high solubility in water (Bolm, 2009). Foremost, it is easily obtainable due to its availability as a

commodity in the commercial. Manual calculations for the preparation of respective iron concentration in cement were computed in Appendix C.

Sample calculation computed that 72.29 grams of iron (III) nitrate nanohydrate was required to yield 10k ppm of iron solution upon dissolving in 1 litre of distilled water. Likewise, the solution containing 30k ppm of iron concentration was prepared via dissolution of 216.95 grams of iron (III) nitrate nanohydrate in 1 litre of distilled water. Paste comprised of respective iron concentration was prepared by mixing iron (III) nitrate nanohydrate with cement in accordance to weight ratio of 1:3, besides same proportion was utilized for the preparation of standard control group 0 ppm in which iron (III) nitrate nanohydrate was excluded. The same procedure was applied for the preparation of cubes which involved RHA as a dopant; 5% weight of RHA was measured as to form specific paste upon mixing in 1 kilogram of cement, subsequently cured.

3.1.3   Preparation of Acetic Acid

In advance, 99.7 wt% of concentrated acetic acid was brought to dilution in order to achieve desirable pH of 2.88 prior to serve as leachate (US EPA, 1986). Accordingly, the exact volume of concentrated acetic acid was defined whereas manual calculations for the preparation of diluted acetic acid was elaborated explicitly in Appendix D.

3.1.4   Preparation of RHA

Brown rice husk can be procured from Malaysia, originated from Kedah paddy field. Rice husk was roasted in a controlled manner, ranging from 550-600˚C via Barnstead Thermolyne 62700 Chamber Furnace, extended to 2 hours and 30 minutes as to eliminate undesirable organic content. Merit to complete combustion, white fluffy ash was observed (Stanley, 2008).

3.2   Whole Block Leaching Procedure

Initially, specific concentration of iron (III) solution obtained via dissolution of iron (III) nitrate nanohydrate in distilled water. Prepared mould in advance, prior to casting. 50 grams of RHA doped upon mixing 1 kilogram of OPC, provided RHA was postulated as a dopant. Subsequently, a solution containing respective iron concentration mixed with OPC to yield paste, primarily cast into cubes. Beakers

containing measured volume of diluted acetic acid solution with a pH set at 2.88 were prepared, preceding leaching procedure was conducted. Leaching process was initiated once hardened solid samples immersed into the solvent, subsequently followed by removal of samples subjected to stipulated durations (US EPA, 1986).

As a whole, constitution and pH present in leachate was testified via performance of inductively coupled plasma optical emission spectroscopy (ICP-OES). Subsequent cement cubes were then introduced to various instruments inclusive of X-ray diffraction (XRD), scanning electron microscope (SEM) as well as energy dispersive X-ray spectroscopy (EDX) aimed to obtain explicit elemental results inherent in cubes.

3.3   Analytical Techniques and Instrumentations

Subsequent to leaching trial, affirmative analysis was performed on both of the aqueous leachate and cement cubes. Aqueous leachate samples subjected to ICP-OES and pH determination, likewise solid samples analyzed via SEM, EDX and XRD procedure. Thence, availability of triplicate values was intended for the leachability control of iron.

3.3.1   X-Ray Diffraction (XRD)

Shimadzu XRD-6000 Diffractometer is a dual modus instrument which capable to justify analysis of sample, chiefly in single crystal structure or pulverized form. Analytical assessment by conducting single crystal technique, aids to elucidate the overall configuration of crystalline material. Conversely, powder diffraction method is conventionally utilized in identification of unknown compounds, associated with comparison of diffraction data against an appropriate database held by International Centre Diffraction Data (ICDD). In addition, appraisal of crystalline compounds in term of crystallographic structure, strains as well as size can be accomplished via powder diffraction (Mehta, 2014). In essence, respective samples were pulverized into powder form in advance, prior to determination of unknown compounds. On account of low sensitivity inherent in XRD, particularly poor detection of tiny or amorphous particles as well as the availability of additional phases (Fultz and Howe, 2013). As a result, EDX is required for elemental analysis.

3.3.2   Scanning Electron Microscope (SEM)

Hitachi S-3400N is a scientific instrument that portrays the image of the specimen via emission of a focused beam of electrons, major in acquiring relevant data regarding topography, morphology, compositional microstructure and crystallographic details. Prior to the performance of SEM test, SC7620 sputter is utilized as to introduce a thin layer of gold coating onto the surface of the specimen. Dispersion of backscattered electrons and formation of auger electrons are the conventional effects, upon interacting between the incident electron beams. Diverse operation modes are employed, aim to achieve desirable information respectively. Instinctively, electron gun serves as a primary generator of the electron source. Electrons which originated from the source generally pass through an aperture of a Whenelt cap, profusely focused via magnetic lens before further projecting onto the sample. Ordinarily, generation of electrons is subjected to relative electrical potential, targets to avoid the probability in causing undesired degradation of samples. Readings indicated at distinct signals are summarized in Table 3.2 (Mehta, 2012).

Table 3.2: Readings Indicated at Distinct Signals

Signals	Details
Backscattered Electron	Atomic Number of Compositional Element
Secondary Electron	Topography of Specimen
Auger Electron	Composition of Specimen
X-ray	Identification of Compositional Element

3.3.3   Inductively Coupled Plasma Optical Emission Spectrometry (ICP-OES)

Optima 7000 DV by Perkin Elmer serves the purpose of standard spectrometry associated with plasma optical emission, functions to evaluate the concentration of metals embedded in a particular solution. In addition, it is capable to analyze all sorts of solution regardless of specificity or availability of multi-element.

Aqueous sample is drawn into a nebulizer at a rate of 1mL/min with the aid of a peristaltic pump. Fine aerosol is produced merit by the presence of argon gas located in the nebulizer, concurrently flows at about 1 L/min. Dispersed droplets of aerosol which composed of 1-2% of the sample are channelled into a spray chamber, primarily ease the separation of fine aerosol from larger droplets. Refined aerosol is

then discharged from the spray chamber subjected to plasma torch via a sample injector (Hou and Jones, 2000).

3.3.4   Leachate pH Determination

Extensively, pH indicator is defined as a designated pH analyzer owing to its capability in the determination of pH lies in respective solution merit to the presence of dual electrodes, namely glass sensor and reference electrode enclosed within a rod-structured probe. A silver chloride filament is embodied in a hollow bulb, naturally saturated in potassium chloride solvent. For simplicity, respective electrodes can be differentiated via aspects of design. The reference electrode is specially formulated by non-conductive glass whereas uniform silica membrane is utilized for fabrication of glass electrode. Readings of the solution are expressed as pH unit, the response in a difference of potential voltage via conversion from an electrical signal. Magnitude of potential voltage is subjected to a distinct gradient in concentration of existing ions, depends on the acidity or alkalinity of the solution. For instance, an increment of hydrogen ions exhibits a high degree of acidity, hence indicates a low value of reading. Yet, high pH reading is observed in response to the availability of hydroxide ions inherent in the alkaline medium. Calibration is performed in advance, necessitate to pH measurement. Ultimately, calibration test can be conducted via submersion of a probe into a prepared buffer solution, subsequently compiled with a standard operating procedure as to verify consistency of measurement. Sufficient immersion of pH probe detects the measure of solvent, extended to an allowable stabilization period up to 5 seconds. Utilization of distilled water as a cleaning agent prior to each measurement, primarily responsible for the removal of undesired impurities. Sartorious pH meter was calibrated under pH of 4, 7 and 10 prior to pH determination (Kahlert et al., 2004).

CHAPTER 4

RESULTS AND DISCUSSION

4.1 X-Ray Diffraction Analysis (XRD)

Commercially available Ordinary Portland Cement (OPC) fundamentally recounted to heterogeneous associations of miscellaneous minerals in vast quantities, namely silicates and aluminates of lime (Zain et al., 2004). Ingression of aqueous solvent rendered the transformation of both CH and C-S-H, successively instigated the dissolution of prominent clinker ($C_2S \& C_3S$). Availability of relative species unambiguously necessitated resolution of XRD to be exploited, essentially upheld the validation of distinctive peaks as visualized in a diffractogram. Derivation of diffraction angle via XRD uniquely granted the resolution of crystallinity, conductively distinguished variant crystallography of constituents inherent in the experimental samples. Characteristic peak attained at a definite angular region by virtue of diffraction, coherently ascertained the presence of discrete functional groups as expressed in Table 4.1 (Mehta, 2014).

Table 4.1: Diffraction Angle at Distinct Minerals

Mineral Phase	2θ
Calcium Hydroxide (CH)	18.07˚ , 34.07˚
Calcium Silicate Hydrate (C-S-H)	29.20˚
Dicalcium Silicate (C_2S)	32.60˚ , 33.25˚
Tricalcium Silicate (C_3S)	32.21˚ , 34.38˚

4.1.1 Overview of XRD Assessment

Pulverization of 100% OPC – 0 ppm Fe and 95% OPC 5% RHA – 0 ppm Fe series in advance, primarily treated as the criterion variables. In either case, both of the criterion groups unequivocally free of ferric ions, either do aqueous solution. Availability of 10k ppm and 30k ppm coexisted in matrix chiefly served as the experimental groups in contemplation of major contextual factors as specified in methodology. For simplicity, relative characteristic peaks shown in diffractogram

justified the distinctive functional groups in reference to search-and-matching models of XRD.

4.1.2 Differential of Contact Duration
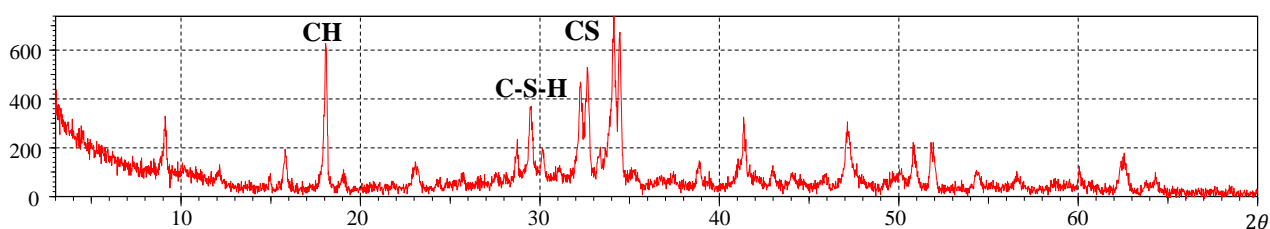
Figure 4.1: XRD Diffractogram of 100% OPC - 10k ppm Fe at 1 h
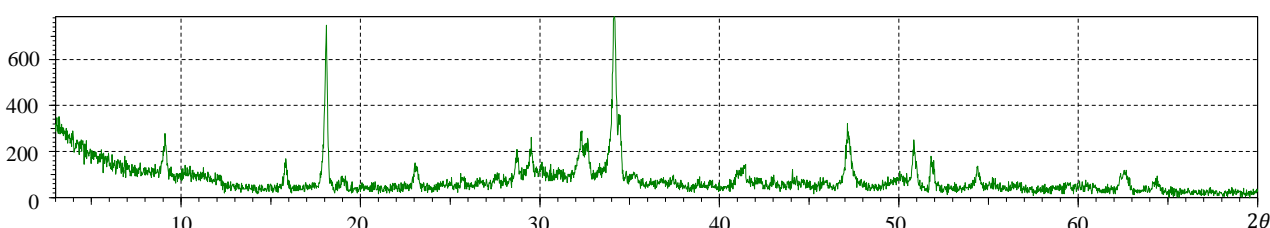
Figure 4.2: XRD Diffractogram of 100% OPC - 10k ppm Fe at 28 days

Table 4.2: Interpretation of Relative Intensity

Sample		CPS (Count Per Second)		
	Duration	CH	C-S-H	CS
100 OPC + 10k Fe	1 h	620	380	500
	28d	740	280	300
95 OPC + 5 RHA + 10k Fe	1 h	540	400	480
	28 d	640	220	280
100 OPC + 30k Fe	1 h	600	400	440
	28 d	700	300	420
95 OPC + 5 RHA + 30k Fe	1 h	580	460	500
	28 d	400	280	340

A detailed diffractogram of XRD expressly denoted several striking similarities in term of definite peaks in effective to 28 days of submersion. Likewise, Table 4.2 extracted the relative intensity of prominent mineral phase existed in each experimental set across stipulated duration.

Reflection angle (2θ) of 18.07° distinctly stood out as the maximal at 28 days, ordinated for the entire experimental group upon valid interpretation of attainable diffractogram as illustrated in Figure 4.2. Diminution of peak likely to be observable in the vicinity of 32.21° as time elapsed, simulation of outcomes duly attributed to

the deprivation of heterogeneous clinkers. Demonstratively, relative abundance of CH outlined the consecutive conversion of C_2S and C_3S merit to prompt dissolution. This principle implied that incessant rate of hydration endorsed the capability for dynamic evolution of CH, albeit to retardation effects at initial curing stage (Janz and Johansson, 2002)

Overall, relative C_2S and C_3S (CS) remarkably upheld an inverse relationship to the synthesis of CH and C-S-H in view of rapid decomposition, incontestably envisaged in declination of peaks as time elapsed.

4.1.3 Differential of Doping Concentration
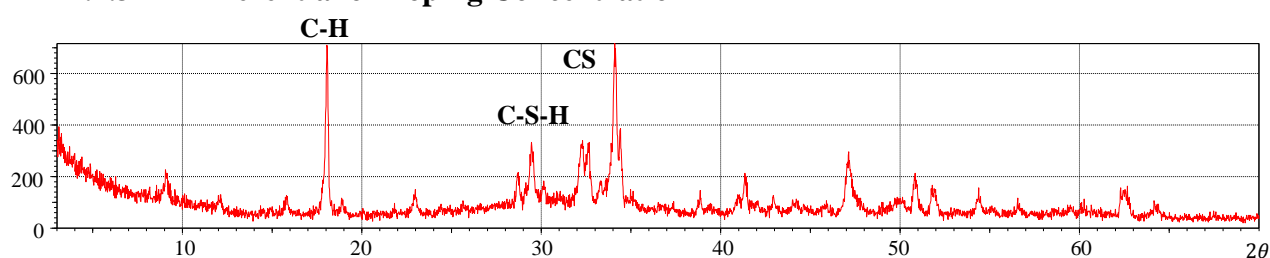
Figure 4.3: XRD Diffractogram of 100% OPC at 7 days for 0 ppm Fe
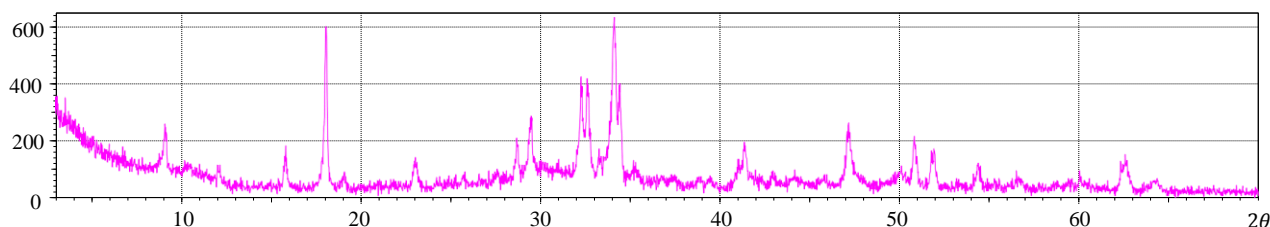
Figure 4.4: XRD Diffractogram of 100% OPC at 7 days for 10k ppm Fe
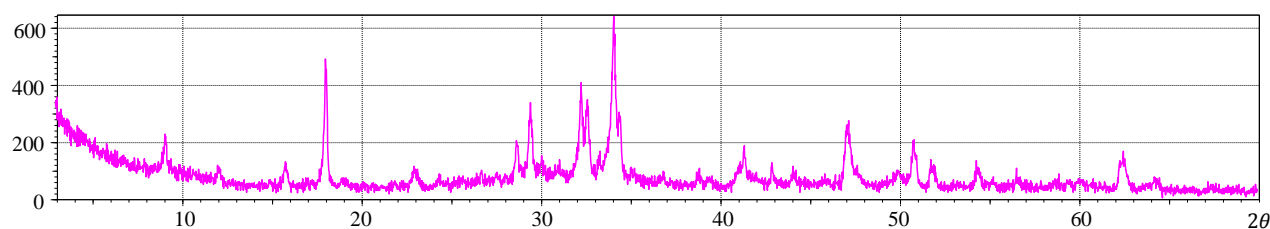
Figure 4.5: XRD Diffractogram of 100% OPC at 7 days for 30k ppm Fe

Simulation of XRD diffractogram of 100% OPC upon 7 days chiefly distinguished relative CPS attributed by discrepancies in concentration. A notable observance of 100% OPC – 0 ppm Fe set as shown in Figure 4.3, evidently constituted the highest overall peak amongst the experimental sets with standing at just 720 CPS. Contrarily, both 10k ppm and 30k ppm accounted for only 600 and 500 CPS as illustrated in Figure 4.4 and 4.5 collectively.

Concentration of ferric ions genuinely expressed an inverse relationship to the productivity of CH. Elevated concentration of ferric ions adversely tolerated limited content of CH as indicated in XRD diffractogram. In contrast, 0 ppm Fe sample positioned a distinct peak of CH on the grounds of ions free condition. Water molecules symbolized as a principal precursor in the process of hydration, unambiguously sustained the exponential growth of CH. Subsequent results implied that concentrated cement samples fundamentally accommodated a lesser volume of water, due to the elevated content of ferric ions under same weight ratio (Sata, 2007).

4.1.4 Differential of Binder Proportion
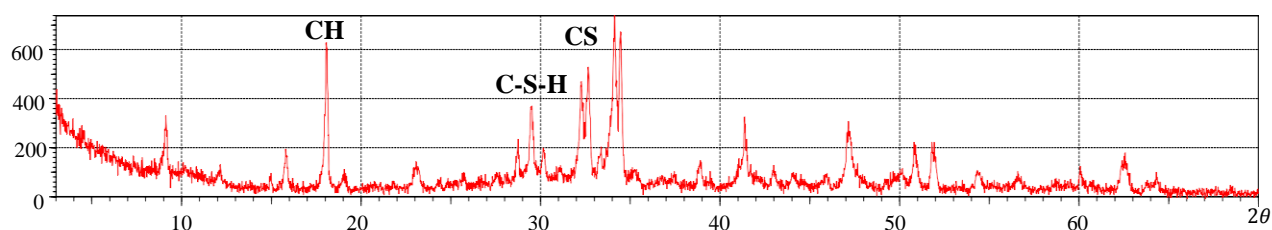
Figure 4.6: XRD Diffractogram at 1 hour for 100% OPC – 10k ppm Fe
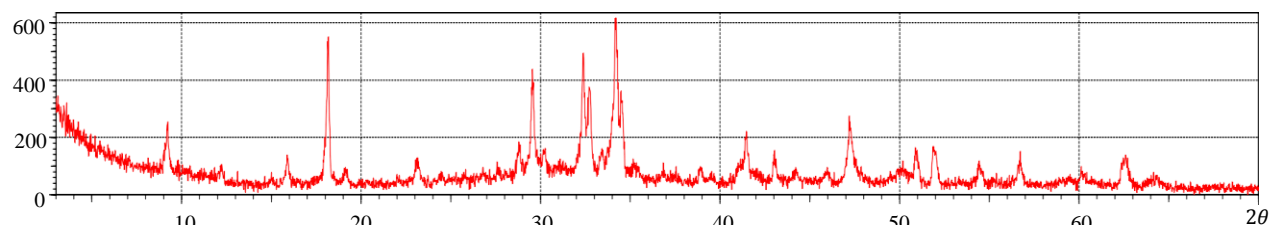
Figure 4.7: XRD Diffractogram at 1 hour for 95% OPC 5% RHA – 10k ppm Fe
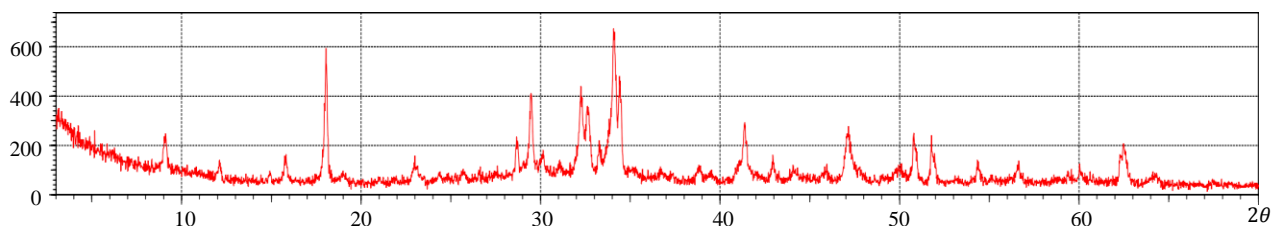
Figure 4.8: XRD Diffractogram at 1 hour for 100% OPC – 30k ppm Fe
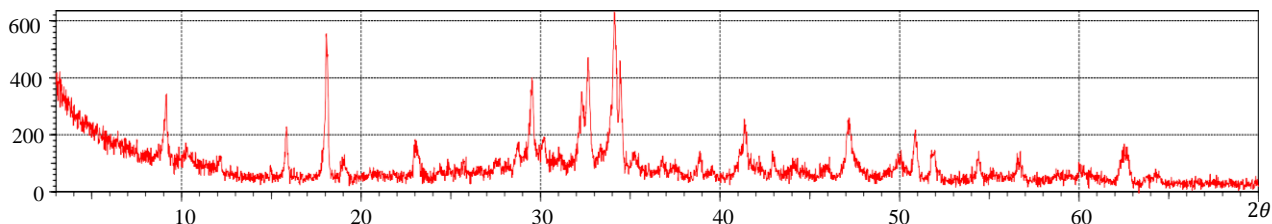
Figure 4.9: XRD Diffractogram at 1 hour for 95% OPC 5% RHA – 30k ppm Fe

A fractional mass of rice husk ash (RHA) served as a pozzolanic admixture merit to its inherently natural silica. Foremost, silica virtually defined as a highly

reactive pozzolanic species enabled the dispersion of secondary C-S-H linkage (Xu et al, 2015).

Availability of 5% RHA in substitution of commercially Ordinary Portland Cement (OPC) signified the reduction of C_2S and C_3S in advance, likely to diminish the evolution of CH to a certain extent as illustrated in Figure 4.7 and 4.9. It has been validated that 100% OPC essentially classified as the major peak in contrast to 95% OPC - 5% RHA, albeit to varying doping concentration. RHA as an alternative apt to instigate the evolvement of C-S-H, successively incurred the depletion of CH as time elapsed. Poorly crystalline of C-S-H intrinsically assigned to a great broadening of diffraction lines in the vicinity of 29.20˚. For simplicity, C-S-H namely categorized as a semi-crystalline phase in phenomena as shown in equation 4.1. Amorphous phase of C-S-H contributed to a broad range of fluctuated diffraction peak, thus unlikely to be detected via XRD (Fultz, 2013).

$$2\,Ca_3SiO_5 + 7\,H_2O \rightarrow 3\,CaO \cdot 2\,SiO_2 \cdot 4\,H_2O + 3\,Ca(OH)_2 \tag{4.1}$$
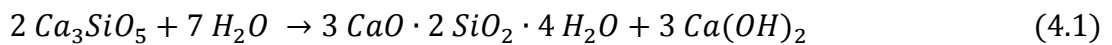
4.1.5 Characterization of Interfacial Deposition

Vast deposition of white solids emerged on the exterior of matrix, majority upon the interfacial phase of leachate. An unambiguous peak allocated at a reflection angle of 29.30, evidently reviewed the crystallinity feature of calcium carbonate $CaCO_3$ as illustrated in Figure 4.10 (Mehta, 2012). Precipitation of calcium carbonate likely to be observable within time frame up to 4 days, predominantly owing to improper sealing of beakers during the experiment. Atmospheric carbon dioxide prompted to experience dissociation, undoubtedly triggered the occurrence of carbonate complexes as shown in equation 4.2 (Robert, 2001).

$$CO_2 + Ca(OH)_2 \rightarrow CaCO_3 + H_2O \tag{4.2}$$
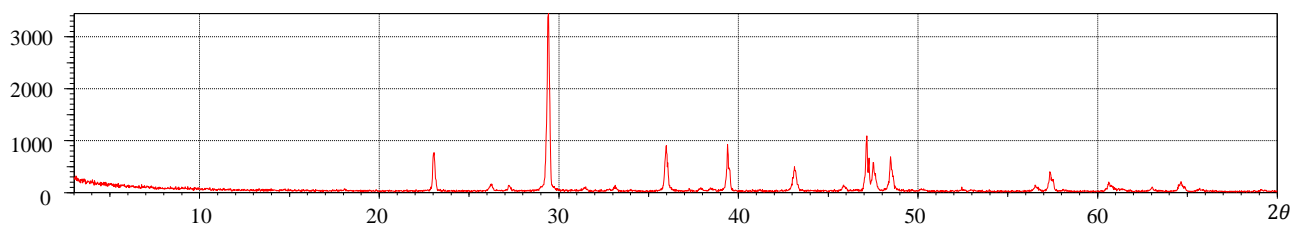
Figure 4.10: XRD Diffractogram of Precipitated White Solid

4.2   Scanning Electron Microscope Morphology (SEM)

Scanning electron microscope (SEM) ascertained the microstructural orientation of essential heterogeneous constituents inherent in solidified matrix, namely contingent upon the density of relative atoms. Brightness of graphic signified the extent of lofty reflection due to the unwrinkled plane condition, likewise murky region adversely imparted to the absorption of reflected wave (Mehta, 2012).

Pellet-like feature of CH arose from the depletion of heterogeneous cement clinker, solely merit to the mechanism of CS hydration. Ettringite prominently assigned to the needle-like appearance by virtue of successive curing process, likewise RHA differentiated as a spherical geometry. Existence of C-S-H characterized by a feature in nanometer scale, potentially instigated the transition of structural phases. Dispersion of miniature crystals ordinated in the inner segment of matrix, primarily susceptible to the agglomeration of suspended hydroxide species (Kogbara et al., 2012).

4.2.1   Morphology of Iron-Contaminated Cement Block
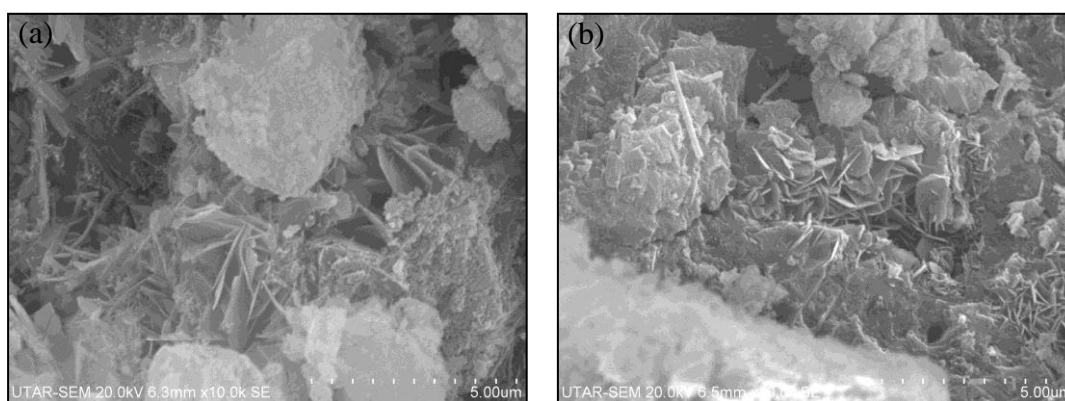
Figure 4.11: Morphology of 100% OPC - 10k ppm Fe upon (a) 1 hour; (b) 28 days

An unequivocal SEM illustration depicted the overarching diverse hydrated species inherent in a heterogeneous cement mixture upon stipulated period of submersion. Irregular topographic surface upon an hour indicated the deterioration of matrix upon initial mixing, chiefly susceptible to availability of acidic species in aqueous state; namely $[Fe(H_2O)_6]^{3+}$ (Hem and Cropper, 1959). Bulk volume of dissolved ferric ions tolerated a limited capacity of water, likely to render the inhibition of hydration reaction; propensity to retarded productivity growth of CH during early hydration as illustrated in Figure 4.11 (a) (Janz and Johansson, 2002).

Ingression of acidic acetic medium adversely incurred the porosity of matrix, preferentially facilitated the leachability of ions to an elevated extent. In turn, a limited dispersion of CH upon an hour outlined the depletion of CH against the acidic condition of solvent by virtue of neutralization. Depletion of unhydrated dicalcium and tricalcium silicate in succession remarkably evoked the advent of abundant calcium hydroxide (Portlandite) upon 28 days as visualized in Figure 4.11 (b). Discrete particulates of tricalcium silicate (Alite) upheld a relatively quiescent period on the basis of initial hydration status, implicitly favoured the synthesis of tenuous pellet-like CH as construed in equation 4.3 (Thomas, 2003).

$$2\ C_3S + 7\ H \ \rightarrow\ C_3S_2H_3 + 3\ CH \tag{4.3}$$
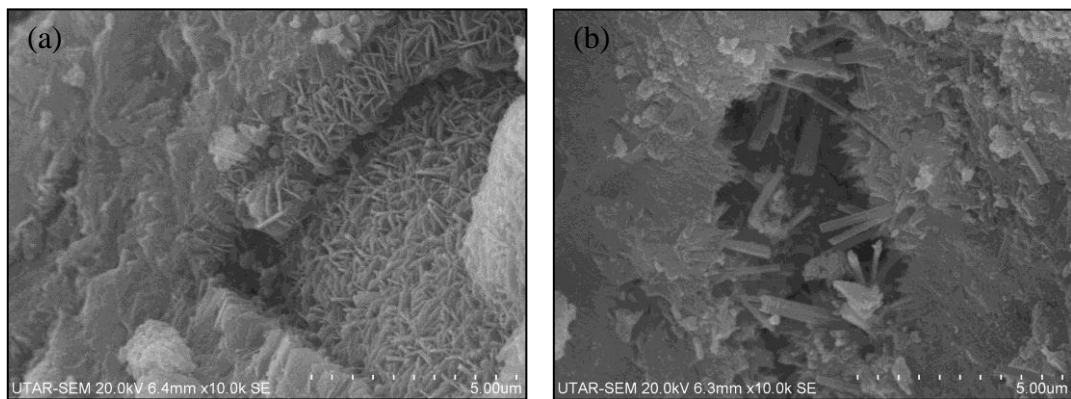
Figure 4.12: Morphology upon 28 days of 10k ppm Fe (a) 100% OPC; (b) 95% OPC 5% RHA

Subsidiary products substantially tolerated an enormous extent of topography as illustrated in Figure 4.12 (a) and (b), primarily the derivation of elongated needle-like calcium sulfoaluminate (Ettringite) upon dissolution of gypsum in the latter times. Localization of insularly dispersed ettringite sufficed void of the matrix, actively endorsed the structural durability of matrix as formulated in equation 4.4 (Sata, 2007).

$$[AlO_4]^- + 3\ [SO_4]^{2-} + 6\ [Ca]^{2+} + aq. \rightarrow C_6AS_3H_{32} \tag{4.4}$$
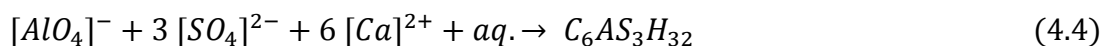
4.2.2 Morphology of Pozzolanic Cement Block
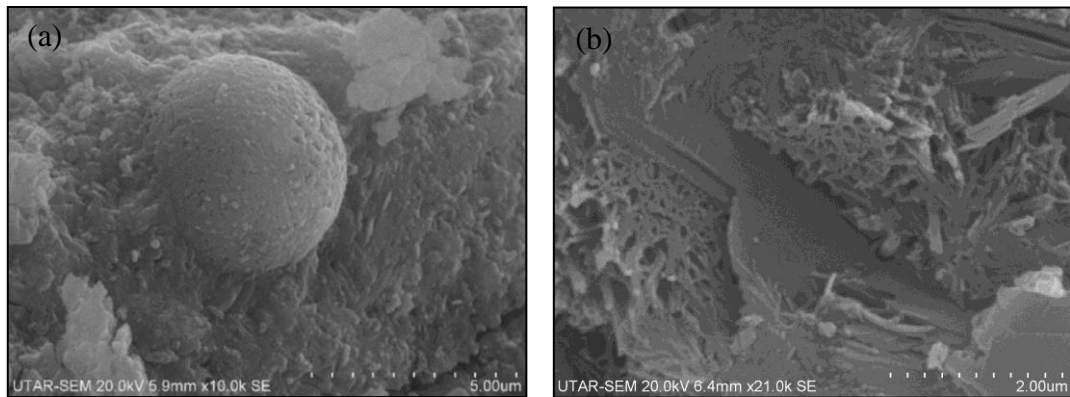
Figure 4.13: Morphology of 95% OPC 5% RHA – 10k ppm Fe upon (a) 1 hour (b) 28 days

Globular protrusion of SEM simulation intrinsically featured the existence of rice husk ash (RHA) as illustrated in Figure 4.13 (a). An elevation in amorphous phase of RHA unambiguously disintegrated into dispersed strains via hydration process as expressed in equation 4.5. Mesh of honey comb likely to be attainable at the early stage, in turn initiated the substantial advancement of interspersed crystallinity morphology. Lamellar hydrated of calcium silicate (C-S-H) implicitly sufficed the penetrability factor of matrix, in effective to several days of nurturement as illustrated in Figure 4.13 (b) (Soares et al., 2015).

$$Al_2Si_2O_7 + Ca(OH)_2 + H_2O \rightarrow C - S - H \tag{4.5}$$
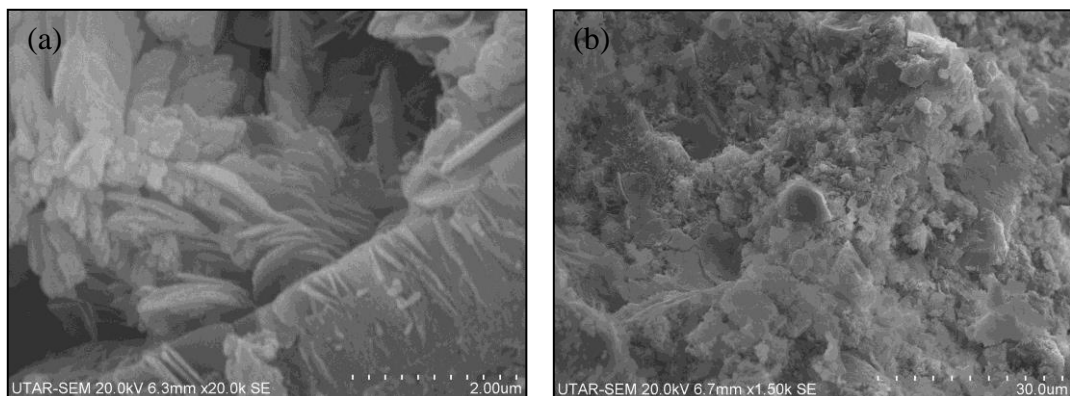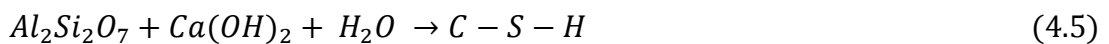
Figure 4.14: Morphology of 95% OPC 5% RHA upon 28 days (a) 10k ppm; (b) 30k ppm

Agglomeration of discrete particulates upheld the evolution of precipitated hydroxide as postulated in equation 4.6, 4.7 and 4.8 upon 28 days of submersion, illustrated in Figure 4.14 (a) and (b) respectively (Frey, 2012). Adsorption of poorly crystallized precipitates in the interstitial phase of the matrix by the aid of C-S-H,

dominantly achieved a limited scale of leaching. S/S matrix indeed formulated an attainable site for immobilization of heavy ions to take place, essentially inhibited the mobility of heavy ions (Anand, 2000).

$$Fe^{2+} + 2\,OH^- \rightarrow Fe(OH)_2 \qquad (4.6)$$

$$Fe(OH)_2 + 2\,H^+ \rightarrow Fe(OH)_3 \qquad (4.7)$$

$$Fe^{3+} + 3\,OH^- \rightarrow Fe(OH)_3 \qquad (4.8)$$

4.3   Energy Dispersive X-Ray Spectroscopy (EDX) Analysis

EDX characterization quantitatively cross-checked the reliability of XRD, foremost authenticated the existence of amorphous precipitates as construed in SEM simulation. Relative abundance of Ca, Si and O elements indeed dominated as the maximal height in contrast with Fe, presumably to be encapsulated as hydroxide complexes in the solidified matrix. Appendix E outlined the exact elemental composition inherent in cement matrix upon stipulated duration.

4.3.1   Characterization of Distinct Contact Time

Table 4.3: EDX of 100% OPC – 10k ppm Fe upon 1 hour, 1 day, 7 days and 28 days

Element	1 hour	1 day	7 days	28 days
Ca (wt %)	58.74	59.53	59.26	61.22
O (wt %)	13.03	16.73	15.45	12.61

Table 4.4: EDX of 95% OPC 5% RHA – 10k ppm Fe upon 1 hour, 1 day, 7 days and 28 days

Element	1 hour	1 day	7 days	28 days
Ca (wt %)	52.59	53.05	54.05	54.30
O (wt %)	15.80	17.33	15.45	16.30

EDX cross-checked the internal and external region of crushed sample, preferentially an evaluation of specific elements inherent in cement block. An inclination of Calcium (Ca) and Oxygen (O) atoms as time elapsed, essentially validated the synthesis of CH as construed in XRD analysis. In contrast, fluctuation of data implied the inconsistence spotting of EDX as tabulated in Table 4.3 and 4.4 respectively.

Ingression of acidic solution inevitably retarded the exterior of matrix, primarily induced the evolution of porosity. Massive dissolution of CH stimulated an elevation in dissociation of Ca and OH ions, hence rendered a limited wt % of Ca and O on the outer region of matrix. A structured inner matrix of cement block indeed invulnerable to the chemical attack of acid, conversely expressed a vast amount of Ca and O elements merit to successive hydration (Mehta, 2012).

4.3.2 Characterization of Distinct Binder Proportion
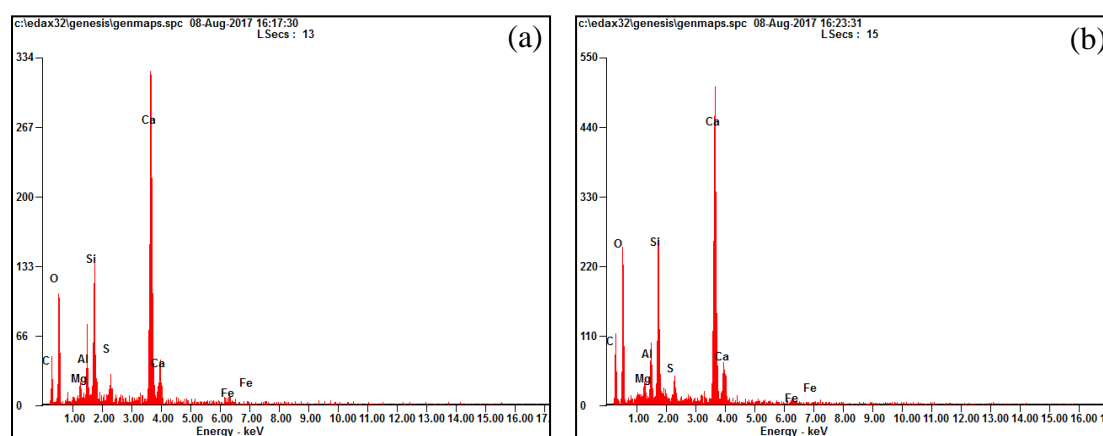
Figure 4.15: EDX simulation of 10k ppm Fe upon 1 hour (a) 100% OPC (b) 95% OPC 5% RHA

Table 4.5: EDX data of 10k ppm Fe upon 1 hour (a) 100% OPC (b) 95% OPC 5% RHA

Element	100% OPC	95% OPC 5% RHA
Ca (wt %)	58.74	52.59
O (wt %)	13.03	15.80
Si (wt %)	14.29	16.65

Elemental Ca assigned as a maximal amongst the detected elements, gradually followed by both Si and O atoms. In turn, Fe species unequivocally stood out as an insignificant fraction in EDX simulation as illustrated in Figure 4.15 (a) and (b). EDX validated the existence of Fe species in the cement block, albeit to trace amount of doping. EDX simulation justified that Fe atom experienced hydroxylation, ultimately adsorbed within the interstitial phase of the matrix (Frey, 2012).

Substitution of 5% RHA promoted a slight increment in Si and O atoms, inversely accounted for a drop in Ca atom. Availability of RHA elucidated the presence of silica (SiO_2), namely constituted of 18-20% of silica (Xu et al., 2015). Depletion of Ca atom successively favoured the productivity of C-S-H, thus resulted in a reduction as time elapsed. Likewise, the loss of 5% primary binder unambiguously denoted a low content of Ca. Table 4.5 outlined the difference in exact weight percent (wt %) of atoms across 1 hour and 28 days of submersion.

4.4 Contemplation of Leachate Concentration (ICP-OES)

Collected leachate extended to stipulated duration transferred to ICP-OES in contemplation of quantitative determination, particularly concentration of iron and calcium existed in leachate. Availability of analytical triplicate samples and standard deviation conditioned by compiled ICP-OES data. Subsequent leachate subjected to dilution prior to analysis, intrinsically facilitated the linear relationship between light intensity along with concentration as illustrated in Figure 4.16.
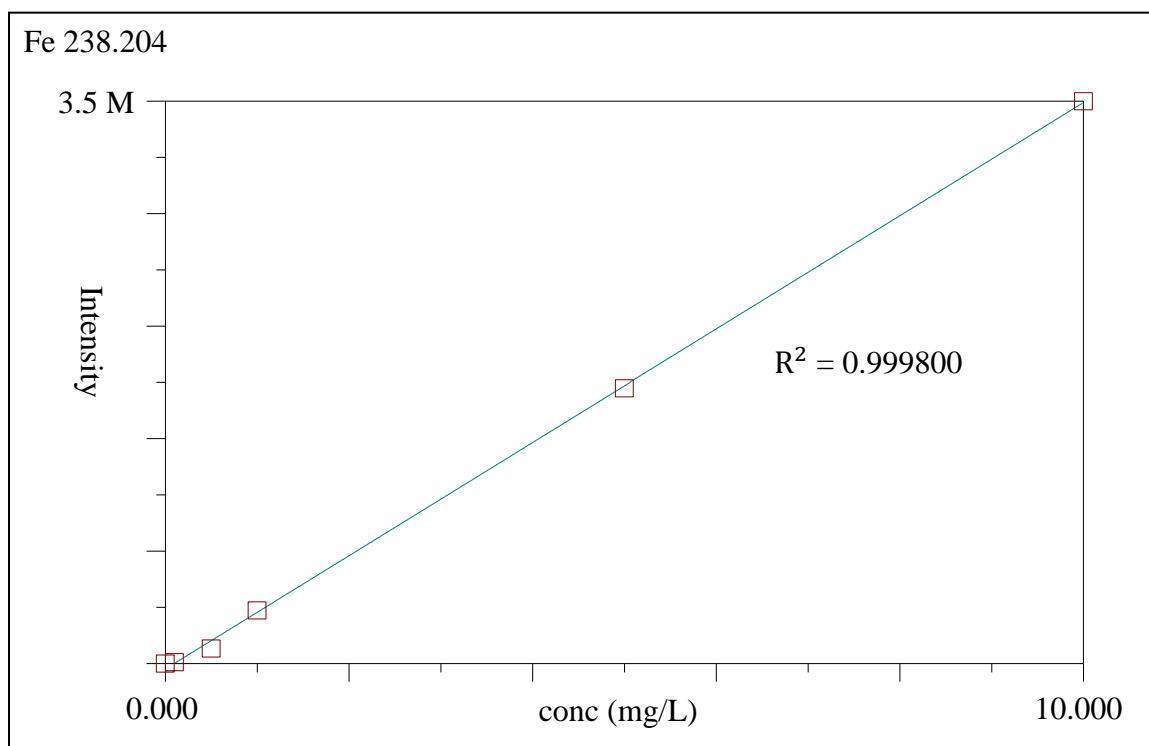
Figure 4.16: ICP-OES Calibration Curve of Iron

Scientifically, Beer's Law proclaimed that concentration of analyte is contingent upon the attenuation of light by virtue of absorption via dissolved constituents in produced solvent. Be in line with Beer's Law, intensity-concentration calibration curve is restrained from linearity subjected to a certain extent of concentration. Thereby, linear relationship is likely to be postulated as definite in respect to low concentration of analyte with coefficient approximate to 1. On the contrary, high concentration of solvent is not favourable as magnitude of intermolecular interactions inherent in analyte are formidable, likely to excite molar absorptivity to be deviated from linearity. Evaluation of successive analysis in beyond the linear boundary, indeed renders the deviation of outcomes (Hou and Jones, 2000). To sum up, calibration curve of iron comprehended by formulated standard of measurements based on 0.001, 0.01, 0.1, 1 and 10 ppm respectively.

4.4.1 Overview of Leaching Assessment

Appendix F summarized the experimental data of monolithic leaching test, highlighted as 100% OPC – Fe subjected to 0k ppm, 10k ppm and 30k ppm. Likewise, 95% OPC 5% RHA – Fe labelled for 0k ppm, 10k ppm and 30k ppm collectively.

4.4.2 Variable Concentration of Iron-Contaminated Leachate
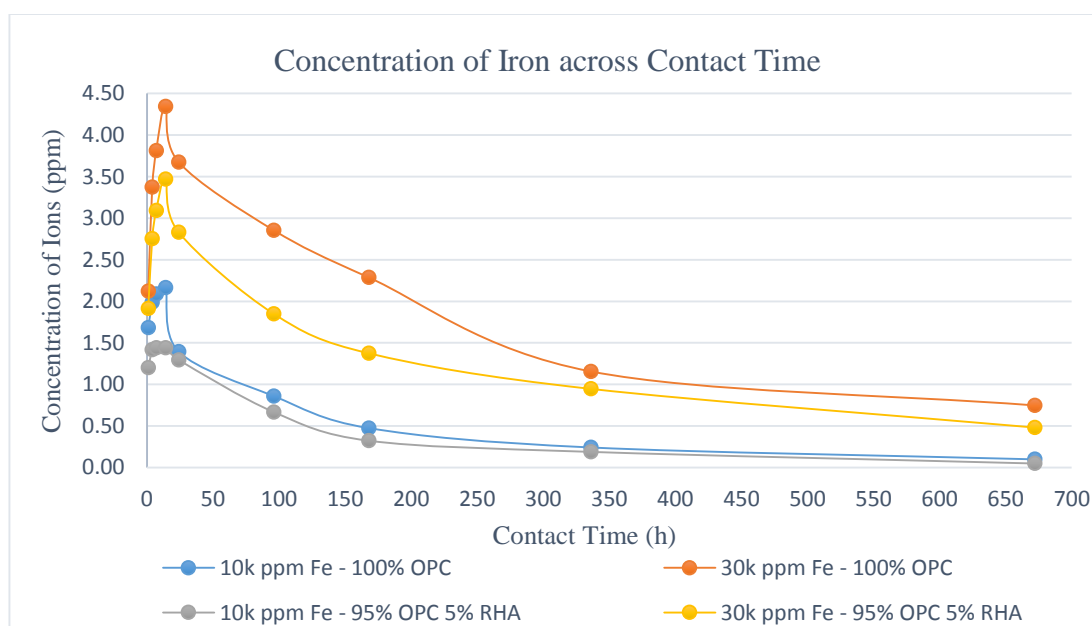
Figure 4.17: Concentration of Iron across Contact Time

Trend analysis of experimental groups unambiguously signified several striking differences as illustrated in Figure 4.17. Concentration of ferric ions collected in leachate increased enormously at the initial stage, essentially exhibited vast declination within time frame up to 24 hours. Contrarily, concentration of ferric ions observed to be levelled off across 28 days and so forth.

According to the given information, both 100% OPC – 30k ppm Fe and 95% OPC 5% RHA – 30k ppm stood out as the highest overall percentage as compared to 100% OPC – 10k ppm Fe and 95% OPC 5% RHA – 10k ppm Fe respectively. Dissociation of ferric ions in 30k ppm doped samples vastly outnumbered 10k ppm, intrinsically facilitated the extent of leaching. This principle postulated as definite, in view of elevated capacity of ferric ions existed in the solidified matrix, albeit to varying dimension.

4.4.3   Disposition of Rice Husk Ash (RHA)

Availability of RHA as pozzolanic additive incessantly exhibited a smaller scale of concentration in contrast to unadulterated OPC as illustrated in Figure 4.17. Incorporation of pozzolans into the cement system certainly retarded the permeability of ferric ions, inevitably instigated the stabilization of ions within the interstitial phase of matrix. C-S-H specially formulated via dissolution of RHA upon consumption of CH as expressed in equation 4.9 (Word Press, 2008).

$$Al_2Si_2O_7 + Ca(OH)_2 + H_2O \rightarrow C - S - H \qquad\qquad (4.9)$$
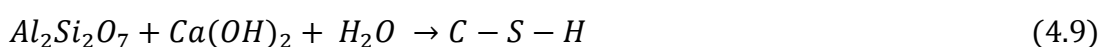
Additionally, C-S-H induced the possibility of lamellar phases in the cement system. Likewise, adjacent pores in solidified matrix likely to be replenished by dint of short fibers. An elevation in evolution of C-S-H compensated the compaction of matrix, preferentially liable to inhibit the leachability of iron (Soares et al., 2015).

4.4.4   Leachability of Iron

Whole block leaching (WBL) procedure took advantage of 10k ppm and 30k ppm as regulatory basis, adherence to criterion endorsed by Ministry of Natural Resources and Environment. Moreover, water-to-binder (w/b) ratio of 0.33 was utilized as to ameliorate the homogeneity of cement paste. In fact, w/b ratio of 0.33 prone to excite

a decent hydration effect, yet likely to inhibit retention of excess moisture in the cement paste (Zain et al., 2004).
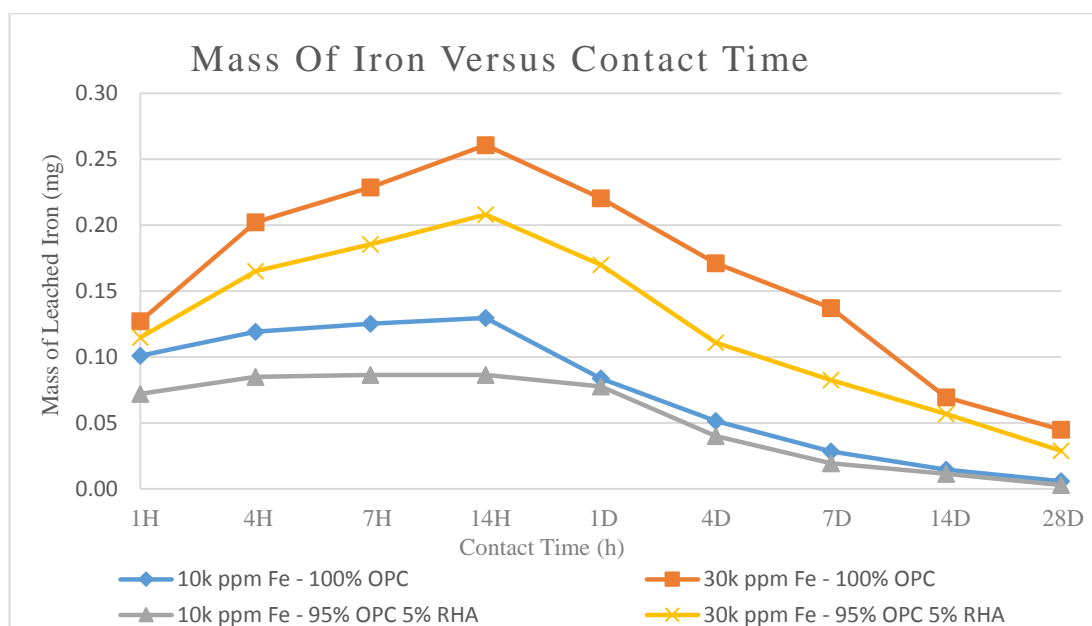
Figure 4.18: Quantity of leached Iron upon 28 days

Figure 4.18 denoted the statistical trends across 100% OPC – 10k ppm Fe, 100% OPC – 30k ppm Fe, 95% OPC 5% RHA – 10k ppm Fe and 95% OPC 5% RHA – 30k ppm Fe upon stipulated duration, chiefly conduced the discrepancies between accumulated mass of iron leached from solidified cubes. 100% OPC – 30k ppm Fe stood out as the maximal, accounted for just 0.261 mg in the vicinity of 14 hours. Moreover, 95% OPC 5% RHA – 30k ppm Fe constituted of only 0.208 mg, predominantly with a slight difference of 0.053 mg. In like manner, 100% OPC – 10k ppm Fe recorded as 0.130 mg at 14 hours, approximately 0.044 mg difference as compared to 95% OPC 5% RHA – 10k ppm Fe. On the contrary, 95% OPC 5% RHA – 10k ppm Fe with 0.003 mg standing at just the minimal upon 28 days, likewise 95% OPC 5% RHA – 30k ppm Fe accounted for 0.029 mg.

Dissertation in contemplation of RHA as pozzolanic admixture pertaining to leachability as accentuated in Figure 4.19. Both statistical trends had risen gradually across the initial stage, extended from hours up to days. Increment of both 10k ppm and 30k ppm RHA-doped specimens validated to be inclined from 0.072 to 0.086 mg and 0.115 to 0.208 mg respectively, ultimately reached a peak at 14 hours.

Substantial decrement of mass observed across 24 hours, accounted for major drops from 0.078 to 0.003 mg and 0.170 to 0.029 mg respectively.
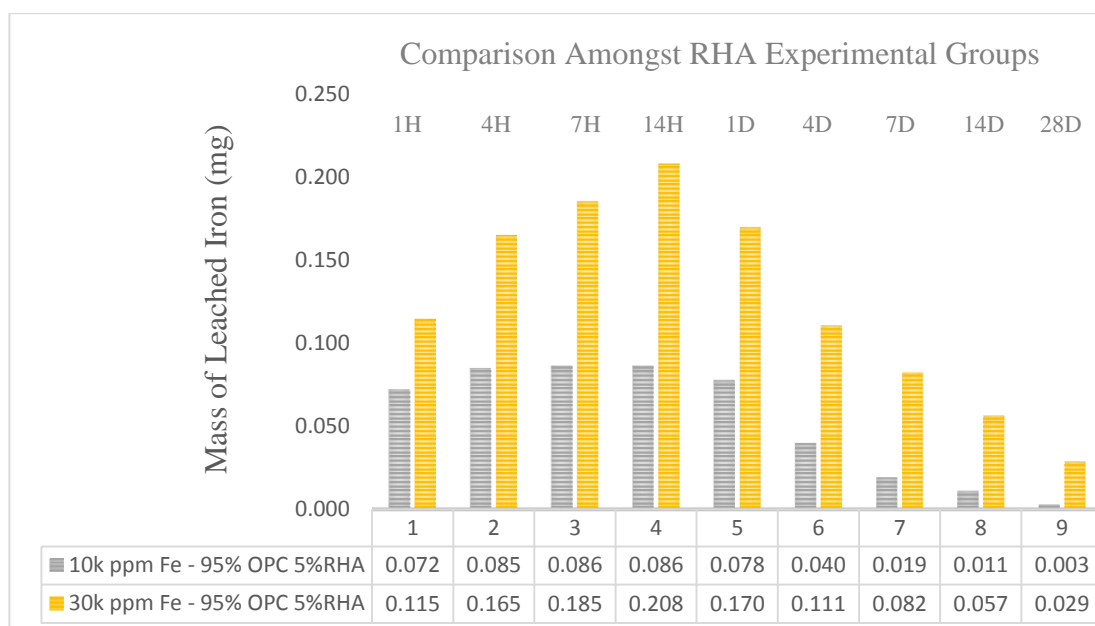
Figure 4.19: Differences between RHA Experimental Groups

On the basis of relevant information, mass of iron likely to be levelled off across 28 days and so forth; mostly clustered between 0.003 mg and 0.029 mg collectively. Subsequent experimental results implied that the presence of C-S-H enhanced the impermeable coating, conjointly with a competency to diminish the hydraulic conductivity of cement as construed in equation 4.9. Hydrated cement induced adsorption of ferric ions within the interstitial phase of matrix, resulted in lower leachability of iron (Xu et al., 2015).

In a nutshell, the effectiveness of OPC as primary binder prior to stimulate the reduction of permeability inherent in ferric ions has been validated via whole block leaching procedure merit to availability of RHA as pozzolanic admixture. Permissible limit of iron below 5 mg/L, indeed adhere to regulatory compliance as affirmed in "A Guide For Investor" (EQA Malaysia, 1974).

4.4.5 Leachability of Calcium

Leaching characteristic of calcium ions unequivocally exhibited several striking similarities to ferric ions as illustrated in Figure 4.20. In general, the concentration of

calcium ions attained its respective peak within short time frame of 24 hours, yet declined progressively to a certain extent.
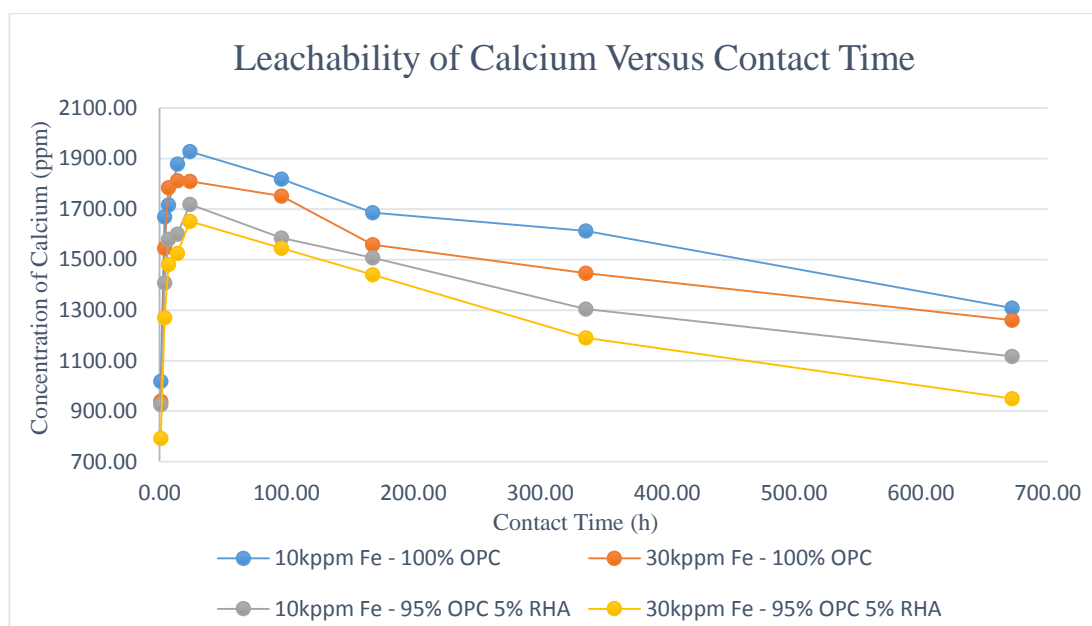
Figure 4.20: Concentration of Calcium Ions across Contact Time

Occurrence of surface erosion in view of exposure to acetic acid, principally exposed inner surface of matrix to chemical attacks. Porosity of matrix essentially excited the leachability of calcium hydroxide via porous region, primarily susceptible to deposition of insoluble calcium carbonate complexes. Incremental slope at initial stage has elucidated that permeability of calcium ions distinctly significant upon 24 hours due to porosity of matrix. Turning now to the disparities, the concentration of calcium had fallen gradually across 96 hours. Appraisal of negative slopes have been validated as definite on the assumption that the degree of deposition rather significant over dissociation of calcium ions (Kogbara and Al-Tabbaa, 2011).

Leachability of RHA doped-samples diminished as opposed to both unadulterated 10k ppm and 30k ppm samples, remarkably exhibited a limited scale of calcium concentration as illustrated in Figure 4.20. This statement postulated as an affirmative, by virtue of the successive hydration between RHA and CH as construed in equation 4.9. Major portions of CH inherent in cement block intrinsically evolved into C-S-H, thus fractions of leachable vastly reduced (Naji, 2010). Appendix G tabulated the exact measure of calcium existed in the leachate.

4.5   Analysis of pH

The extent of ions mobility highly dependent on the ambience conditions, hence pH reckoned as the basic contextual factor in contemplation of leachability studies. For simplicity, Appendix H outlined the triplicate results of pH.

4.5.1   Variable pH of Leachate
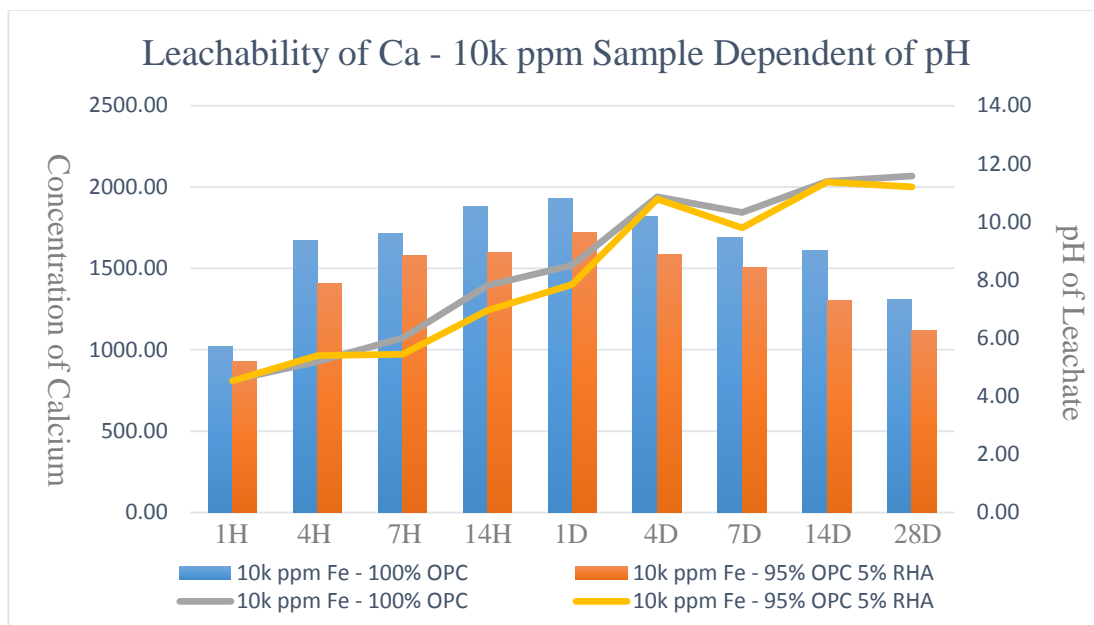
Figure 4.21: Leachability of Ca - 10k ppm Sample across pH changes
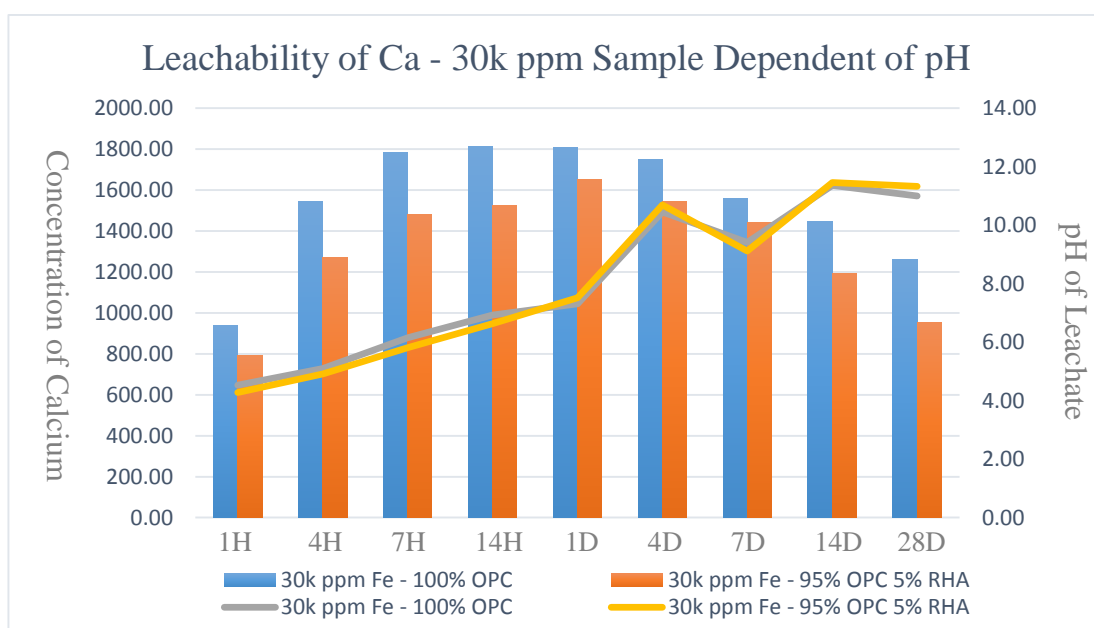
Figure 4.22: Leachability of Ca - 30k ppm Sample across pH changes

Statistical trends of pH followed a similar pattern at respective initial stage, essentially inclined in a gradual manner across stipulated duration as illustrated in Figure 4.21 and 4.22 respectively. Neutralization initiated upon contacting solidified cement cubes with acidic leachate, successively reached an equivalence point at a certain period. Fractional dissociation of CH due to short period of hydration, weakly suppressed the acidic characteristic of acetic acid at the early stage. Cloudy appearance of leachate indicated the dissolution of CH, inevitably gave rise to elevated accumulation of calcium and hydroxyl ions (Kogbara et al., 2012). In turn, prompt dissociation of CH signified the successive increment of pH across 96 hours. Decrement of hydrogen ions inherent in acidic leachate via neutralization, essentially contributed to alkalinity of solvent. A notable increment of pH ranged from 2.88 right up to 7, merit to sufficient neutralization.

pH accounted for 7 days of submersion, denoted as an outlier for respective experimental groups as illustrated in Figure 4.21 and 4.22 respectively. Each of the plastic beakers enclosed with a finite head space, accommodated capacity of carbon dioxide to a limited extent in the closed system. Dissolution of aqueous carbon dioxide inevitably stimulated the reduction of hydroxyl ions in the system, chiefly favoured the forward reaction in return for the advent of carbonic acid. Evolution of carbonic acid competent to promote acidity of leachate, primarily susceptible to evolution of carbonate intermediates. Huge portions of carbonate and bicarbonate ions profusely attained, granted for the accretion of hydrogen ions as expressed in equation 4.11 and 4.12 (Stanley, 2008). Thus, consumption of hydroxyl ions in vast quantities resulted in inflection of pH.

$$CO_2\ (aq) + H_2O + OH^- \rightarrow H_2CO_3 \tag{4.10}$$

$$H_2CO_3 \rightarrow HCO_3^- + H^+ \tag{4.11}$$

$$HCO_3^- \rightarrow CO_3{}^{2-} + H^+ \tag{4.12}$$

Carbonation mechanisms exhibited dynamic properties merit to condition of ambience as illustrated in Figure 4.23. Carbonate equilibrium favoured the evolution of bicarbonate ions at pH ranged from 6 to 10, likewise dissociation of carbonate ions enhanced over pH of 10. Saturation of leachate prohibited successive dissociation of CH, likely to retain pH at around 9 (Bolm, 2009).
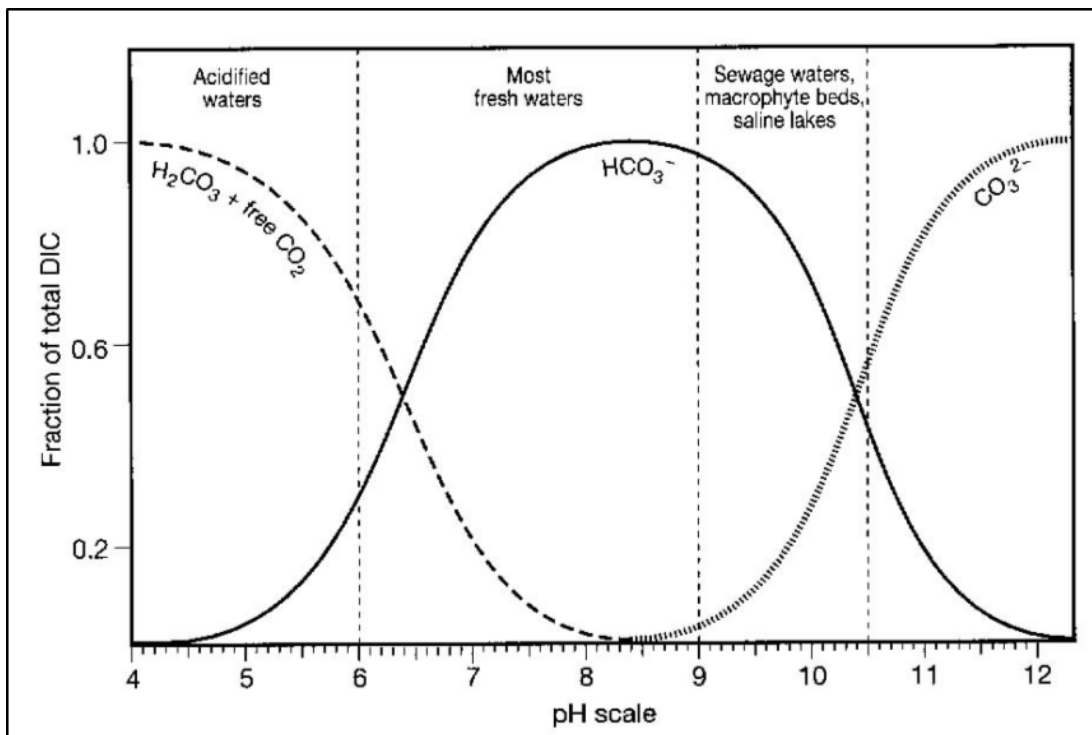
Figure 4.23: Carbonate Equilibrium

Excess calcium ions subsequently gave rise to calcium bicarbonates, owing to low extent of dissociated carbonate ions. Carbonate ions restored upon establishment of carbonate equilibrium, enabled the conversion of soluble calcium bicarbonate to insoluble calcium carbonate. Desaturation of calcium ions in leachate liable to successive dissolution of CH across 168 hours, principally signified the inclination of leachate pH. Equation 4.13 and 4.14 expressed the hydrolysis pathways of calcium carbonate (Bolm, 2009).

$$CaCO_3 \leftrightarrow Ca^{2+} + CO_3{}^{2-} \qquad (4.13)$$
$$CO_3{}^{2-} + HOH \leftrightarrow HCO_3{}^- + OH^- \qquad (4.14)$$

Alkalinity of leachate likely to be levelled off up to time frame of 350 hours and so forth due to the elevated level of carbonate complexes. High mobility of calcium ions possessed a preeminent tendency to form respective carbonate complexes, accounted for the production of calcium carbonate and calcium bicarbonate. 10k ppm Fe sample signified the major leachability of calcium, merely outnumbered respective experimental groups as illustrated in Figure 4.21. This finding justified the ample hydration of cement, on the grounds that elevated amount

of calcium ions formed in the cement cubes. Vast quantities of calcium ions capable of undergoing calcination, principally liable to the formation of calcium carbonate. This principle postulated as definite, merit to the deposition of white precipitates on the exterior of specimens as well as the interfacial phase of leachate.

Turning now to the differences, both 10k ppm and 30k ppm RHA-doped samples exhibited a much lower scale of pH value. Elevated capacity of ferric ions competed with calcium ions at this stage, predominantly migrated from inner matrix via diffusion and dissolution. Modest dissociation of calcium ions in the system unlikely to excite the saturation of carbonate complexes, nor shifted the carbonate equilibrium. This statement implied that accumulated capacity of ferric ions existed in the leachate opted to favour hydroxylation, subsequently gave rise to accumulation of iron hydroxide (Frey, 2012).

4.5.2 Immobilization of Metal Ions

Immobilization of naturally occurring iron merit to precipitation, essentially susceptible to be levelled off in the latter times. Leachability of iron principally exhibited a local pH dependency, albeit to several chemical aspects. Dissociation of ions dominant under acidic condition, readily gave rise to elevated amount of mobile ferric ions. Redox activity of iron oxide fundamentally favoured the evolution of ferrous ions as shown in equation 4.15. Vice versa, iron embedded in cement cubes may arise in the form of insoluble ferric hydroxide at elevated level of alkalinity as expressed in equation 4.17, 4.18 and 4.19 respectively (Hem and Cropper, 1959). Moreover, iron complexes likely to be entrapped within the S/S matrix via matrix adsorption (Malviya and Chaudhary, 2006). Foremost, it has been elucidated that mobility of ions highly dependent on local pH as illustrated in Figure 4.24 and 4.25.

$$Fe_2O_3 \leftrightarrow 2\,Fe^{3+} + Fe^{2+} + 4\,O^- \tag{4.15}$$

$$Fe(NO_3)_3 \leftrightarrow Fe^{3+} + 3\,NO_3^- \tag{4.16}$$

$$Fe^{2+} + 2\,OH^- \rightarrow Fe(OH)_2 \tag{4.17}$$

$$Fe(OH)_2 + 2\,H^+ \rightarrow Fe(OH)_3 \tag{4.18}$$

$$Fe^{3+} + 3\,OH^- \rightarrow Fe(OH)_3 \tag{4.19}$$

As a whole, pH of leachate greatly dependent on the dynamic equilibrium lied between calcium and carbonate intermediates. Neutralization occurred at the early stage, ultimately stabilization of pH owing to saturation of CH and calcium carbonate in the latter times.
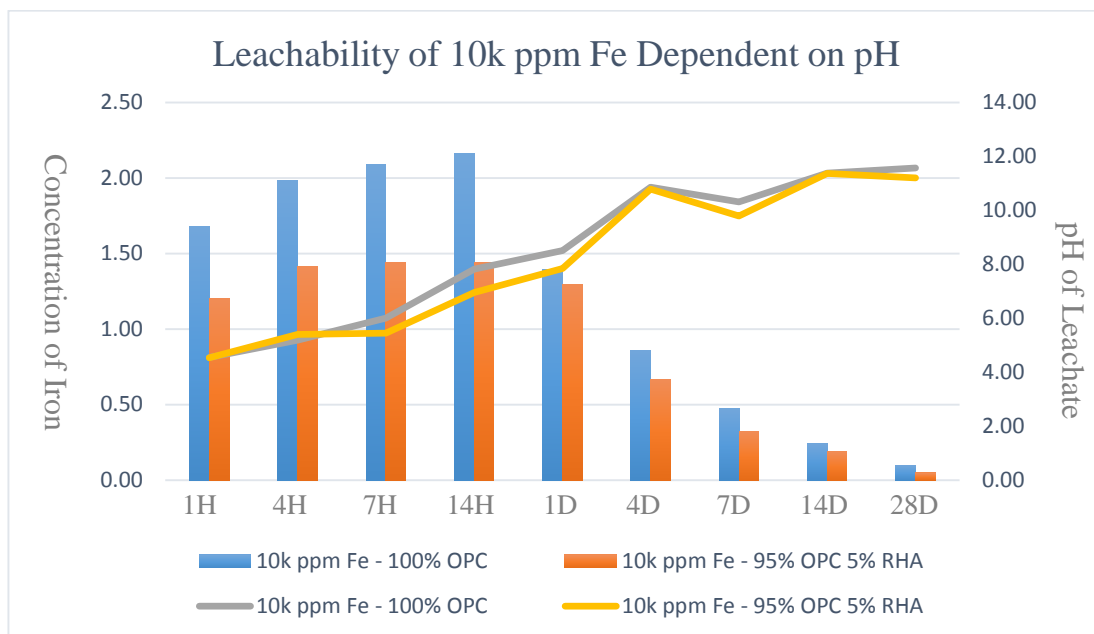
Figure 4.24: Leachability of 10k ppm Fe across pH changes
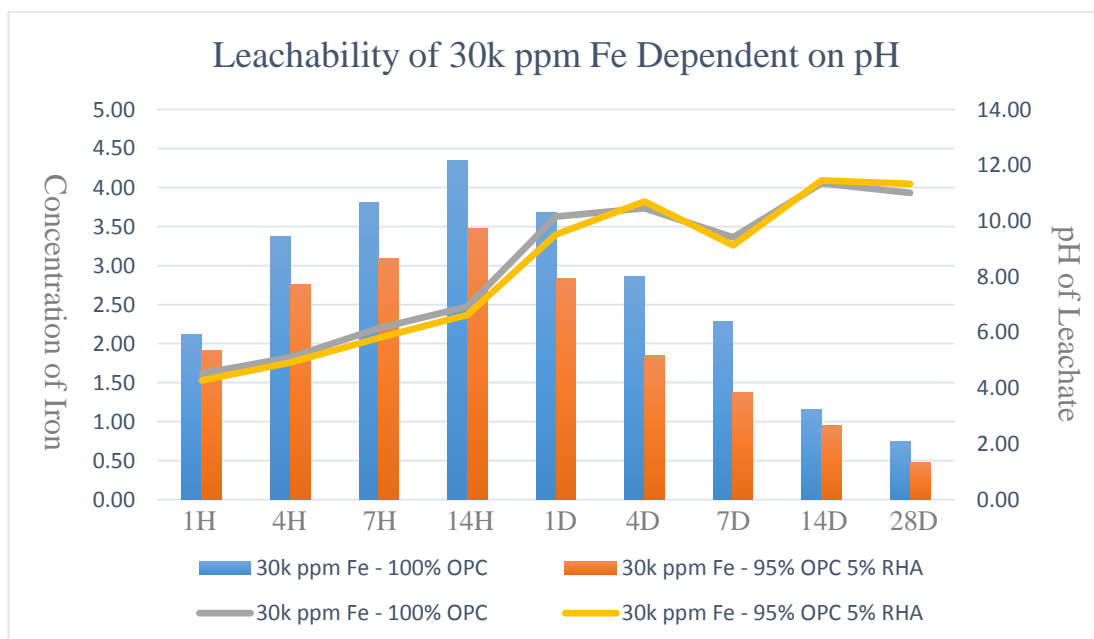
Figure 4.25: Leachability of 30k ppm Fe across pH changes

CHAPTER 5

CONCLUSION AND RECOMMENDATIONS

5.1   Conclusion

The overarching objective of this study is to evaluate the contextual factors of leachability coupled with the availability of rice husk ash (RHA) as pozzolanic admixtures. Whole Block Leaching test (WBL) is accustomed to leaching activity across 28 days, intends to initiate the leachability of iron contingent upon relative variable. Integrated experimental results are validated via extensive analytical techniques and instrumentations, ideally accuracy and reliability of data are likely to be achievable.

Analysis of concentration inherent in leachate accomplished via ICP-OES, liable to quantitative determination of ions. Permeability of both iron and calcium denoted a similar pattern, literally signified a major increment at the early stage. Concentration of iron essentially stood out as a maximal in the vicinity of 14 hours, whereas calcium accounted for 24 hours. A minor declination unambiguously observable for either parties within time frame up to 4 days, subsequently reached a constant in the latter times. It has been elucidated that an elevated dissociation of ions merit to concentrated-doped samples, remarkably facilitated the extent of leaching.

Gradual increment of pH at the initial stage merit to prompt neutralization reaction between acidic acetic acid solution and dissociated calcium hydroxide (CH). Finite head space of system tolerated a fractional amount of atmospheric gaseous, in turn aqueous carbon dioxide favoured the advent of carbonic acid upon dissolution across 7 days. Accretion of both bicarbonate and carbonate ions indeed altered the equilibrium of carbonate cycle, adversely induced a slight decrement of pH. Saturation of leachate inhibited successive dissociation of CH, inevitably gave rise to accumulation of calcium bicarbonate at pH 9. Reversible activity of bicarbonate and carbonate ions excited the restoration of carbonate equilibrium via consumption of carbonate ions, extended from 7 days to 14 days. Elevated deposition of several insoluble hydroxides and carbonates gave impetus to the alkalinity of leachate, likely to be levelled off across 28 days of submersion. Dynamic equilibrium of

intermediates generalized the local pH of leachate, likewise subsequent results implied that mobility of ions affirmatively exhibited an appreciable pH dependency.

Alkaline cement cubes possessed vulnerability to acidic leachate, ultimately resulted in porosity of matrix. Retarded interior part of cement matrix unequivocally observable via scanning electron microscopy (SEM), primarily susceptible to chemical attacks. SEM virtually displayed the microstructural features of constituents, specifically ettringite, CH, C-S-H and RHA. Experimental results indicated an incremental deposition of crystalline solids on exterior of specimens, subjected to extended periods of submersion.

Potentiality of Ordinary Portland Cement (OPC) as a primary binder in treating the leachability of ferric ions, essentially stimulated the immobilization of ions within the interstitial phase of matrix. X-ray diffraction (XRD) analysis performed as to spectacle the capability of RHA in exciting the transformation of calcium silicate hydrate (C-S-H). It has been elucidated that availability of RHA apt to facilitate the reduction of calcium concentration in produced solvent, likewise evolution of C-S-H incurred the successive depletion of calcium hydroxide (CH) as time elapsed. EDX enabled the qualitative analysis of element species existed in cement matrix, namely hydroxide and oxide form of iron.

As a conclusion, availability of OPC coupled with RHA as an additional admixture relatively instigated the immobilization of ions via high structural integrity. S/S technique fairly ascertained the feasibility of disposal by virtue of a cost-effective alternatives, reliably stimulated the elimination of heavy metals. A comprehensive schematic preparatory procedure for cement cubes as attached in Figure 5.10, likewise Figure 5.20 expressed a detailed mechanism of leachability. Leachability limit of iron as below of 5 mg/L indeed satisfied the regulatory limit as adherence to "A Guide For Investor".

Ordinary Portland Cement (OPC)

Rice Husk Ash (RHA)

Ferric Nitrate Solution

Preparatory Procedure for Cement Cubes

❖ Homogeneous cement paste was obtained via dissolution of ferric nitrate solution in OPC, introduction of additional 5 wt% RHA for respective sample

❖ Transfer of cement paste into a 25 mm x 25 mm x 25 mm mould prior to compaction and casting purpose

❖ Cured cement cube was demolded upon 24 hours, subjected to analytical testing

Monolithic Leaching Procedure

❖ Submersion of solidified cubes into a sealed plastic beaker upon contact with acidic medium, extended to stipulated duration

❖ Drying of cement cubes via desiccator prior to morphological analysis

❖ Storage of collected leachate in a centrifuge tube, eased the quantitative determination of analyte

Diluted Acetic Acid Solution

Cubes

Leachate

XRD and EDX

• Pulverized sample subjected to XRD and EDX analysis

✓ To study the microstructural features of constituents

✓ To determine the elemental species of sample

SEM

• A section of sample inspected via SEM

✓ To evaluate the morphological structure of constituents

pH

• Measurement of pH justified via pH analyzer

✓ To investigate the pH dependence inherent in leaching behaviour

ICP-OES

• A fractional volume of leachate introduced to ICP-OES

✓ To verify the concentration of analyte present in produced solvent

Figure 5.1: Experimental Flow Chart
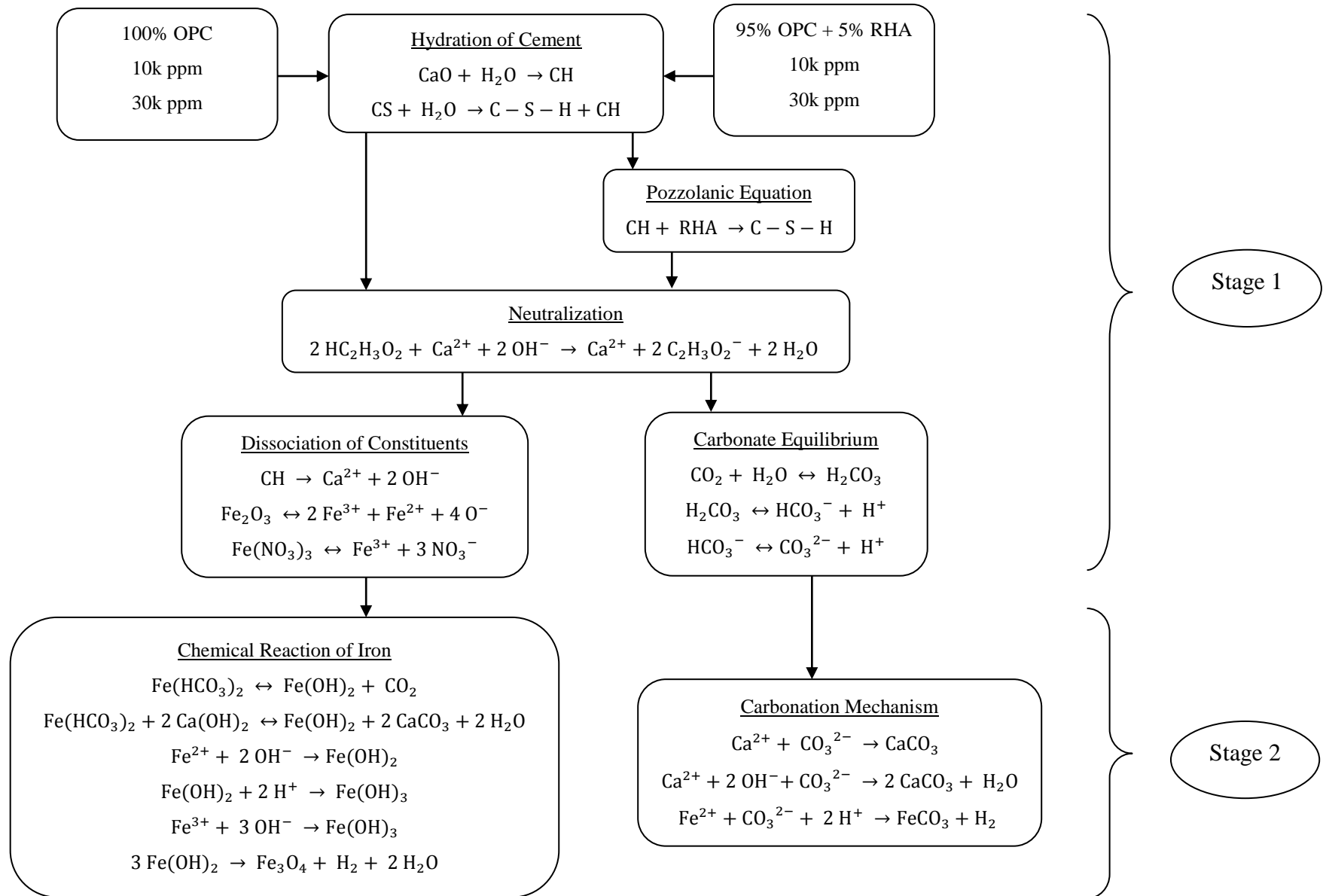
Figure 5.2: Leachability Mechanism

5.2   Limitations and Recommendations

Measurement of experimental results in term of reliability, precision and accuracy is achievable by virtue of proper operating procedure and recommendations. Significant contextual factors and uncertainties inherent in this research indeed necessitate a few modifications and improvements to be formulated.

Whole Block Leaching Procedure (WBL) ordinarily accustomed to short-term leaching studies, unlikely to simulate the landfill conditions effectively in contrast to Toxicity Characteristic Leaching Procedure (TCLP). Utilization of unadulterated ferric compound coupled with acetic acid as an acidic medium, ironically incapable of imitating real landfill condition. Industrial waste is recommended as a source of experiment, conducive to manipulate the leachability of ferric ions. Availability of miscellaneous metal ions inherent in industrial waste conversely excites the behaviour of ferric ions to a certain extent as opposed to an unadulterated ferric compound. In succession, the effectiveness of protic solvent as medium is apt to be accomplished via appreciable aspects in term of normal or acidic rain (US EPA, 1992).

The effect of mould deformation has stood out as a major concern during the process of casting. The inherent flexibility of cardboard mould is potentially vulnerable to the dynamic actions of fluid, primarily susceptible to rupture of mould. Likewise, exertion of a non-uniform pressure by the fluid on the wall of mould adversely obstructs the overall structure and sustainability of cast cubes. Cast cement cubes are likely to be deviated from preferred geometry due to relevant aspects, essentially result in volumetric shrinkage. It is evident that inconsistent surface orientation of cast cubes undoubtedly affects the accuracy and precision of experimental results. Dimensional variation of mould necessitates appropriate treatment to be exploited, as to devise reliable design of mould prior to casting. Perspex acrylic sheet is recommended as mould design merit to its distinctive properties in term of strength, stability, reusability as well as permeability. Sustainable geometry of specimens formulated by Perspex fairs to inhibit the leakage of cement paste, in turn improves the productivity of uniform cast cubes.

Compressive strength of cement cubes is customarily subjected to the magnitude of w/b ratio, likely to induce a variation of consolidated shear strength inherent in the cement block. In fact, such alterations in strength substantially

necessitates unconfined compression test to be performed. Measurement of unconfined compressive strength prioritizes the disposal of cement cubes into the environment, principally adhere to prerequisite requirements of the landfill. Thereby, it is essential to introduce various proportions of RHA in contemplation of leachability as to justify the validation of experimental outcomes. Current study signifies the reduction of calcium content in leachate, extended to certain level of reduction indeed remain unsolved. Existence of additional iron prone to act as an inhibitor of endurance, fundamentally exhibits deleterious impact on the strength of cement cubes. Deliberately, availability of RHA promotes the durability of cement cubes merit to its distinctive cementitious properties. Silica content of RHA enables the loss of endurance ought to be compensated, likewise responsible for the reduction of permeability of constituents (Naji, 2010).

New innovative techniques are devised practically ease the analysis of concentration, thus the gap between quantitative determination and ionic characterization are expected to widen. Ion chromatography test is recommended, conducive to identification of iron species in produced solvent. Variation of retention time by ion chromatography generally implies the differential charges inherent in both ferrous and ferric ions. Likewise, characterization of iron enable the appraisal of risk assessment affiliated with iron-bearing contaminant (Mehta, 2012).

Ideally, subsequent recommendations are proposed for validation and extension of environmental methods.

REFERENCES

Anand J. R., Krishna R. P. and Arun S. W., 2000. Stabilization and solidification of metal-laden wastes by compaction and magnesium phosphate based binder. *Journal of the Air & Waste Management Association, (50) 9*, 1623-1631.

Anbar, A.D., 2004. *'Iron stable isotopes: Beyond biosignatures', Earth and Planetary Science Letters, 217(s 3–4),* 223–236

Bobby Miller, 2014. *The facts on recycling, electric vehicles, and solar energy.* Retrieved from http://nvate.com/16744/americans-greener.html

Bolm, 2009 *'A new iron age: Abstract: Nature chemistry'*, Nature Chemistry, 1(5), 420

Carsten, B., Tino, K., Markus, S., Aristi, P., Fernandes, Margareta, R., Edgren and Ulf, T., Brunk, 2010. *Chelation of lysosomal iron protects against ionizing radiation, Biochemical Journal*, (432), 2, 295-301.

Chaychian, M., Al-Sheikhly, M., Silverman, J. and McLaughlin, W.L., 1998. *'The mechanisms of removal of heavy metals from water by ionizing radiation', Radiation Physics and Chemistry, 53(2)*, pp. 145–150

Chen J.J., Thomas J.J., Taylor H.F.W. and Jennings H.M., 2004. *Solubility and structure of calcium silicate hydrate*. Taylor Memorial Issue.

Connolly, E.L. and Guerinot, M.L., 2002. *'Iron stress in plants', 3(8).*

Dickinson and Robert E., 1964. *Germany: A regional and economic geography (2nd ed.). London*: Methuen.

El-Moselhy, K.M., Othman, A.I., El-Azem, A.H. and El-Metwally, M.E.A., 2014. *'Bioaccumulation of heavy metals in some tissues of fish in the red sea, Egypt', Egyptian Journal of Basic and Applied Sciences, 1(2),* pp. 97–105

European Commission, 2002. *Heavy Metals in Waste*. Retrieved from: http://ec.europa.eu/environment/waste/studies/pdf/heavy_metalsreport.pdf

Cotton and Wilkinson ,1988. *Advanced Inorganic Chemistry, Wiley Interscience, New York*

Fu and Wang, 2011. *Journal of Environmental Management 92*, pp 407-418

Frey, P.A., Reed and G.H., 2012. *'The ubiquity of iron', ACS Chemical Biology, 7(9)*, pp. 1477–1481

Fultz, B., Howe and J.M., 2013. *Transmission electron microscopy and diffractometry of materials. 4th ed. Heidelberg*: Springer-Verlag Berlin.

Garbarino, J.R., Hayes, H., Roth, D., Antweider, R., Brinton, T.I. and Taylor, H., 1995. *Contaminants in the Mississippi river. U. S. Geological Survey Circular, Virginia, U.S.A.*, pp 1133.

Garrison, S. and Times, T.D., 2017. *Gold king mine spill a disaster waiting to happen.* Retrieved from: https://www.abqjournal.com/628976/gold-king-mine-spill-a-disaster-waiting-to-happen.html

Gräfen, H.; Horn, E. M.; Schlecker, H. and Schindler, H., 2000. *"Corrosion".* Ullmann's Encyclopedia of Industrial Chemistry. Wiley-VCH.

Grazuleviciene R, Nadisauskiene R, Buinauskiene J and Grazulevicius T., 2009. *Effects of Elevated Levels of Manganese and Iron in Drinking Water on Birth Outcomes.* Polish J of Environt Study 18(5), pp 819–825

Gutenberg, P., 2013. *Project Gutenberg self-publishing.* Retrieved from: http://www.gutenberg.us/articles/iron-gall_ink

Hem J.D. and Cropper W.H., 1959. *Survey of Ferrous-ferric Chemical Equilibria and Redox Potentials.* US Geological Survey Water-Supply Paper 1459-145A

Hou, X. and Jones, B.T., 2000. Inductively couple plasma/optical emission spectrometry in *Encyclopedia of Analytical Chemistry.* Meyers, R.A. (ed.), pp. 9468-9485.

Istomin, V.E. and Duchkov, A.D., 2008. *'Iron ions Fe2+ and Fe3+ in a magnetic model of the sedimentary medium', Izvestiya, Physics of the Solid Earth, 44(5),* pp. 421–426

James J. and Stephen M. T., 2004. *Overview of chromium (VI) in the environment: background and history.* Boca Raton: CRC Press.

Jan De Vries, 1994. *The Journal of Economic History Vol. 54, No. 2,* Papers Presented at the Fifty-Third Annual Meeting of the Economic History Association pp. 249-270

Janz, M. and Johansson, S., 2002. *The function of different binding agents in deep stabilization.* Sweden: Swedish Deep Stabilization Research Centre.

Jensen, K.P. and Ryde, U., 2004. *'How O2 binds to Heme', Journal of Biological Chemistry, 279(15),* pp. 14561–14569.

Kahlert, H. et al., 2004 *'A new calibration free pH-probe for in situ measurements of soil pH', Electroanalysis, 16(24),* pp. 2058–2064.

Kasassi, A., Rakimbei, P., Karagiannidis, A., Zabaniotou, A., Tsiouvaras, K., Nastis, A. and Tzafeiropoulou, K., 2017. *'Soil contamination by heavy metals: Measurements from a closed unlined landfill',* Bioresource Technology, 99(18), pp. 8578–8584

Kim, S.A. and Guerinot, M.L., 2017. *'Mining iron: Iron uptake and transport in plants', FEBS Letters,* 581(12), pp. 2273–2280

Kogbara, R.B. and Al-Tabbaa, A., 2011. *Mechanical and leaching behaviour of slag-cement and lime-activated slag stabilised/solidified contaminated soil. Science of The Total Environment,* 409(11), pp.2325-2335.

Kogbara, R.B., Al-Tabbaa, A., Yi, Y and Stegemann, J.A., 2012. *pH-dependent leaching behaviour and other performance properties of cement-treated mixed contaminated soil. Journal of Environmental Sciences,* 24(9), pp. 1630-1638.

Kolasinski, Kurt W., 2002. *"Where are Heterogenous Reactions Important".* Surface science: foundations of catalysis and nanoscience. John Wiley and Sons. pp. 15–16

Kosaka, F., Hatano, H., Oshima, Y. and Otomo, J., 2015. *'Iron oxide redox reaction with oxide ion conducting supports for hydrogen production and storage systems',* Chemical Engineering Science, 123, pp. 380–387

Lewin, S.A. and Wagner, R.S., 1953. *'The nature of iron(III) thiocyanate in solution', Journal of Chemical Education,* 30(9), p. 445

LibreTexts, C., 2013. *Oxidation-reduction reactions.* Retrieved from: https://chem.libretexts.org/Core/Analytical_Chemistry/Electrochemistry

Malviya, R. and Chaudhary, R., 2006. *Leaching behavior and immobilization of heavy metals in solidified/stabilized products.* Journal of Hazardous Materials, 137(1), pp. 207-217.

Mehta, P.K. and Monteiro, P.M.J., 2014. *Concrete: microstructure, properties and materials.* 4th ed. New York: McGraw-Hill Education

Metha, R., 2012. *Interactions, imaging and spectra in SEM. In: Kazmiruk, V., ed. 2012.* Scanning Electron Microscopy. Intech, pp. 17-30.

OSHA, 2014. *Metal & Metalloid particulates in workplace atmospheres.* Retrieved from: https://www.osha.gov/dts/sltc/methods/inorganic/id121.html

Naji, Givi et al., 2010. *Contribution of rice husk ash to the properties of mortar and concrete*: a review. J. Am. Sci. 6 (3), 157–165.

U. S. Environmental Protection Agency, 2001. *National Primary Drinking Water Regulations; Arsenic and Clarifications to Compliance and New Source Contaminants Monitoring*; Final Rule 66: 14, 6976-7066.

Papanikolaou, G. and Pantopoulos, K., 2005. *'Iron metabolism and toxicity', Toxicology and Applied Pharmacology*, 202(2), pp. 199–211

Philip L. H., 2004 'Use of Short-Term (5-Minute) and Long Term (18-Hour) Leaching Tests to Characterize, Fingerprint, and Rank Mine Waste Material from Historical Mines in the Deer Creek, Snake River, and Clear Creek Watersheds in and around the Montezuma Mining District, Colorado. U.S. Geological Survey Scientific Investigations Report.

Robert D., 2001. Solidification and stabilization treatment. Paper presented at the Cement Association of Canada, Remediation Technology Workshop. Canada, Toronto. May 2001.

Sabbas and Polettini, 2003. Management of municipal solid waste incineration residues, Volume 23, Issue 1, Pages 61-88

Sata, V., Jaturapitakkul, C. and Kiattikomol, K., 2007. Influence of pozzolan from various by-product materials on mechanical properties of high-strength concrete. Constr. Build. Mater. 21 (7), 1589-1598.

Siemiatycki, J., Richardson, L., Straif, K., Latreille, B., Lakhani, R., Campbell, S., Rousseau, M.-C. and Boffetta, P., 2004. 'Listing occupational carcinogens', 112(15).

Skoog, D. A., West, D. M., Holler, F. J. and Crouch, S. R., 2004. Fundamental of analytical chemistry. Eighth Edition. Belmont: Brooks/Cole.

Soares, L.W.O., Braga, R.M., Freitas, J.C.O., Ventura, R.A., Pereira, D.S.S. and Melo, D.M.A., 2015. The effect of rice husk ash as pozzolan in additive to cement Portland class G for oil well cementing. Journal of Petroleum Science and Engineering, 131, pp. 80-85.

Stanley E. M., 2008. Fundamentals of Environmental Chemistry. Third Edition. Boca Raton: CRC Press.

Tangahu, Voijant, B., Abdullah, S., Rozaimah, S., Basri, H., Idris, M., Anuar, N. and Mukhlisin, M., 2011. 'International journal of chemical engineering', International Journal of Chemical Engineering

Teien, Garmo OA, Atland A and Salbu B, 2008. Transformation of iron species in mixing zones and accumulation on fish gills. Environmental Sciences and Technology 42, 1780–1786.

Thomas J.J., Chen J.J., Neumann D.A. and Jennings H.M., 2003. Ca–OH bonding in the C–S–H gel phase of tricalcium silicate and white portland cement pastes measured by inelastic neutron spectroscopy. Chem. Mater, 15, pp. 3813–3817.

Timothy S. G. and Jane G., 2001. Ten things to know about Minamata disease. Japan: The Minamata Environmental Creation Development.

Tokar E. J., Boyd W. A., Freedman J. H. and Wales M. P., 2013. "Toxic effects of metals", in C. D. Klaassen (ed.), Casarett and Doull's Toxicology: the Basic Science of Poisons, 8th ed., McGraw-Hill Medical, New York, ISBN 978-0-07-176923-5

Toyokuni, S., 2002. *Iron and carcinogenesis: from Fenton reaction to target genes*. Redox Rep. 7, 189– 197.

US EPA, 1986. *Whole Block Leaching Procedure*; 1986, 51, 216.

US EPA, 1992. Method 1311, Toxicity Characteristic Leaching Procedure (TCLP). Publication SW−846: *Test Methods for Evaluating Solid Waste, Physical/Chemical Methods.* Retrieved from: www. epa.gov/epaoswer/hazwaste/test/pdfs/1311.pdf

US EPA, 2000. *In situ treatment of soil and groundwater contaminated with chromium. Technical Resource Guide. Cincinnati*: Office of Research and Development Washington.

US EPA, 2001. *Solidification/Stabilization. Resource Guide*. Cincinnati: Office of Research and Development Washington.

Volesky, B., Sears, M., Neufeld, R.J., and Tsezos, M., 1983. *Recovery of strategic elements by biosorption*. pp. 310

WHO, World Health Organization, 1996. *Trace elements in human health and nutrition. Chapter 3: Trace element bioavailability and interactions*. Geneva. pp. 23-41.

WordPress, 2008. *Rice husk ash (Thailand).* Retrevied from: http://www.ricehuskashthailand.com/rice-husk-ash-products

Xu, W., Lo, Y.T., Ouyang, D., Memon, S.A., Xing, F., Wang, W. and Yuan, X., 2015. *Effect of rice husk ash fineness on porosity and hydration reaction of blended cement paste*. Journal of Construction and Building Materials, 89, pp. 90-101.

Yoshihisa, Y., Shimizu, T. and Hindawi, 2012. *Dermatology Research and Practice*, pp 8

Zain, M. F. M., Islam, M. N., Radin, S. S. and Yap, S. G., 2004. *Cement-based solidification for the safe disposal of blasted copper slag*. Cement & Concrete Composites. 26, pp. 845-851.

Zhang, Y.-Q., Dringen, R., Petters, C., Rastedt, W., Köser, J., Filser, J. and Stolte, S., 2016. *'Toxicity of dimercaptosuccinate-coated and un-functionalized magnetic iron oxide nanoparticles towards aquatic organisms'*, Environmental Science: Nano, 3(4), pp. 754–767

APPENDICES

APPENDIX A: Overview Pathways of Waste Stream

Waste Generation Facility   **Off-site Facilities**

Y **Shipped off-site** (Expl. 1)

Off-site Waste Management Facilities

Y+ **Processing of Listed or Characteristic Waste that is subject to LDR** (Expl. 3)

Y **Shipped off-site** (Expl. 1 and Expl. 2)

Residue

N **Processing (Waste not subject to LDR)** (Expl. 4)

Y **Shipped off-site** (Expl. 1)

Residue

Y **Waste Disposal** (e.g., Landfill, Thermal Treatment, Waste Derived Fuel) (Expl. 5)

Generating Process

Residue (e.g., combustion ash, leachate)

Y* **OWRA Facility (Wastewater Treatment)** Only hazardous waste discharges to final stage require registration (Expl.6)

N **Water course**

Residue

Y* **Discharge to Sanitary Sewers** (Expl. 7)

Off-Site Water Pollution Control Plants (WPCP) Municipal OWRA Approved (Expl. 8)

Y **Shipped off-site** (Expl. 1)

Y **Storage** (e.g., PCB waste, subject waste stored more than 2 years) (Expl. 9)

N **Residue**

N - No Registration Required
Y - Subject Waste Registration Required
Y+ - Registration is only required if the processed waste or the residual from processing the waste is still a subject waste
Y* - Only hazardous waste registration required

Any of the above on-site waste management activities producing wastes (sludge, skimmings, etc.) become generating facilities and the resulting wastes may be subject to registration based on destination.
Small quantity exemptions apply to all of the above situations.

APPENDIX B: Toxicity Characterization

Is the waste Severely Toxic? (Expl. 1) — No →

Is the waste Pathological? (Expl. 2) — No →

Is the waste a PCB waste as defined by Regulation 362? (Expl. 3) — No →

Is the waste an Acute Hazardous Waste Chemical? (Expl. 4) — No →

Is the waste an Hazardous Waste Chemical? (Expl. 4) — No →

Is the waste an Hazardous Industrial Waste? (Expl. 5) — No →

Is the waste Ignitable, Corrosive or Reactive? (Expl. 6, 7, 8, 10) — No →

Is the waste Leachate Toxic? - Schedule 4 Criteria (Expl. 9, 10) — No →

Yes ↓

Characterization Listed
-Severely Toxic

- Schedule 3

(S)

No SQE

Yes ↓

Characterization
-Pathological

(P)

No SQE

Yes ↓

Characterization
-PCB Waste

(D)

Yes ↓

Characterization Listed
-Acute Hazardous Waste Chemical
- Shedule 2 Part A

(A)

SQE = 1 kg/mo.

Yes ↓

Characterization Listed
- Hazardous Waste Chemical
- Schedule 2 Part B

(B)

SQE = 5 kg/mo.

Yes ↓

Characterization Listed
- Hazardous Industrial Waste
- Schedule 1

(H)

SQE = 5 kg/mo.

Yes ↓

Characterization Characteristic

- Ignitable (I)
- Corrosive (C)
- Reactive (R)

- Schedule 5

SQE = 5 kg/mo.

Yes ↓

Characterization Characteristic
- Leachate Toxic

- Schedule 5

(T)

SQE = 5 kg/mo.

Start

Subject to Generator Registration Requirements. (See Figure 4)

Waste is not a Subject Waste. Generator Registration is not Required.

Characterization
- Decharacterized with Untreated UHCs
(U)

The waste is a Hazardous Waste. The first Characterization is the Primary Characterization.

Characterization
- Liquid Industrial Waste
(L)
SQE = 25 L/mo.

Is the waste a Liquid Industrial Waste? (Expl. 12) — Yes →

Is the waste a Decharacterized Waste with Untreated UHCs? (Expl. 10) — No → , Yes ↑

Does your waste have one or more of the Hazardous Waste Characterizations? (Expl. 11) — Yes ↑ , No →

APPENDIX C: Preparatory Calculation of Iron Nitrate Solution

Calculation of 10k ppm Fe^{3+} (Stanley, 2008)

Doping concentration of Fe^{3+} ions	: 10000 mg/L
Molecular weight of Fe	: 55.8450 g/mole
Molecular weight of O	: 14.0067 g/mole
Molecular weight of N	: 15.9994 g/mole
Molecular weight of Fe $(NO_3)_3 \cdot 9\ H_2O$	: 403.8453 g/mole

Iron (III) Nitrate; Fe $(NO_3)_3 \cdot 9\ H_2O$:

$$= (55.8450) + (3)[(14.0067) + (3)(15.9994)] + (9)[(2)(1.00) + (15.9994)]$$

$$= 403.8543\ \frac{g}{mole}$$

Parts per million (ppm) is equivalent to mg/L;

10k ppm of Fe in solution:

$$= \left(10\text{ x }10^3\ \frac{mg}{L}\right) \times \frac{(1.0\text{x}10^{-3})\ g}{mg} \times \frac{mole\ Fe^{3+}}{(55.8450)\ g}$$

$$= 1.79\text{ x }10^{-1}\ \frac{mole\ Fe^{3+}}{L}$$

Iron (III) Nitrate, Fe $(NO_3)_3$ required:

$$= 1.79\text{ x }10^{-1}\ \frac{mole\ Fe^{3+}}{L} \times \frac{403.8543\ Fe(NO_3)_3\ \cdot\ 9\ H_2O\ g}{mole\ Fe^{3+}}$$

$$= 72.29\ \frac{Fe(NO_3)_3\ \cdot\ 9\ H_2O\ g}{L}$$

Hence, **72.29 g** of Fe $(NO_3)_3 \cdot 9\ H_2O$ yield 10k ppm of ferric ions upon dissolution in 1 L of distilled water.

Calculation of 30k ppm Fe^{3+} (Stanley, 2008)

Doping concentration of Fe^{3+} ions   : 30000 mg/L

Molecular weight of Fe   : 55.8450 g/mole

Molecular weight of O   : 14.0067 g/mole

Molecular weight of N   : 15.9994 g/mole

Molecular weight of Fe $(NO_3)_3 \cdot 9\ H_2O$: 403.8453 g/mole

Iron (III) Nitrate; Fe $(NO_3)_3 \cdot 9\ H_2O$:

$$= (55.8450) + (3)[(14.0067) + (3)(15.9994)] + (9)[(2)(1.00) + (15.9994)]$$

$$= 403.8543\ \frac{g}{mole}$$

Parts per million (ppm) is equivalent to mg/L;

30k ppm of Fe in solution:

$$= \left(30\ x\ 10^3\ \frac{mg}{L}\right) \times \frac{(1.0x10^{-3})\ g}{mg} \times \frac{mole\ Fe^{3+}}{(55.8450)\ g}$$

$$= 5.372\ x\ 10^{-1}\ \frac{mole\ Fe^{3+}}{L}$$

Iron (III) Nitrate, Fe $(NO_3)_3$ required:

$$= 5.372\ x\ 10^{-1} \frac{mole\ Fe^{3+}}{L} \times \frac{403.8543\ Fe(NO_3)_3\ \cdot\ 9\ H_2O\ g}{mole\ Fe^{3+}}$$

$$= 216.95\ \frac{Fe(NO_3)_3\ \cdot\ 9\ H_2O\ g}{L}$$

Hence, **216.95 g** of Fe $(NO_3)_3 \cdot 9\ H_2O$ yield 30k ppm of ferric ions upon dissolution in 1 L of distilled water.

APPENDIX D: Preparatory Calculation of Acetic Acid Solution

Acetate and hydronium ions arose upon dissociation of acetic acid in medium as shown in stoichiometric equation (Skoog et al., 2004).

$$CH_3COOH + H_2O \leftrightarrow CH_3COO^- + H_3O^+$$

Equilibrium constant stated as:

$$K = \frac{[CH_3COO^-][H_3O^+]}{[CH_3COOH][H_2O]}$$

Partial dissociation of acetic acid can be expressed as;

$$HA \rightarrow H^+ + A^-$$
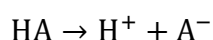
Where;

HA denotes as acetic acid,

H^+ denotes as cationic hydrogen,

A^- denotes as anionic acetic acid,

K_α denotes as dissociation constant of acid at 25°C

In reference to Skoog et al., 2004;

K_α approximately equals to 1.75×10^{-5}, whereas pH is assumed as 2.88

$pH = -\log[H^+]$

$[H^+] = 10^{-2.88}$

$[H^+] = 1.318 \times 10^{-3}$ mol/L

Hence, concentration of acetic acid can be termed as;

$$K_\alpha = \frac{[H^+][A^-]}{[HA]}$$

$$\alpha = \frac{(1.318 \times 10^{-3})^2}{1.75 \times 10^{-5}} + 1.318 \times 10^{-3}$$

$$\alpha = 0.100 \text{ mol/L}$$

Purity of stocked acetic acid   : 99.7 wt%

Molecular weight of acetic acid   : 66.052 g/mol

Density of acetic acid   : 1.05 g/cm^3

Concentration of stocked acetic acid

$$= \frac{99.7 \text{ g } CH_3COOH}{100 \text{ g solution}} \times \frac{\text{mol } CH_3COOH}{60.052 \text{ g } CH_3COOH} \times \frac{1.05 \text{ g solution}}{cm^3 \text{ solution}} \times \frac{1000 cm^3}{1 \text{ L}}$$

$$= 17.432 \text{ mole } CH_3COOH/L$$

Dilution of concentrated acetic acid solution:

$$M_1 V_1 = M_2 V_2$$

$$V_1 = \frac{M_2 V_2}{M_1}$$

$$V_1 = \frac{0.100 \text{ M } (1000 \text{ ml})}{17.432 \text{ M}}$$

$$V_1 = 5.737 \text{ ml}$$

Thus, **5.737 ml** of stocked acetic acid yield pH of 2.88 upon dilution in 1 L of distilled water.

APPENDIX E: EDX Results of Cement Block

Sample		Contact Duration (hour)			
	Element	1	24	168	672
100% OPC + 0k ppm Fe	Ca	65.14	67.69	62.82	64.75
	O	15.27	12.88	16.79	14.08
	Si	13.04	13.25	13.91	14.28
	Fe	N/A	N/A	N/A	N/A
95% OPC + 5% RHA 0k ppm Fe	Ca	54.05	59.42	74.36	50.37
	O	23.38	8.74	8.38	13.70
	Si	14.77	12.98	12.22	5.18
	Fe	N/A	N/A	N/A	N/A
100% OPC + 10k ppm Fe	Ca	58.74	59.53	59.26	61.22
	O	13.03	16.73	15.45	12.61
	Si	14.29	14.89	15.33	15.78
	Fe	2.58	2.34	2.65	2.35
95% OPC + 5% RHA 10k ppm Fe	Ca	52.59	53.05	54.05	54.30
	O	15.80	17.33	15.45	16.30
	Si	16.65	17.89	18.11	18.49
	Fe	2.38	2.11	3.52	3.14
100% OPC + 30k ppm Fe	Ca	53.89	54.01	54.24	54.71
	O	18.72	17.43	18.56	19.30
	Si	16.80	17.21	15.77	15.79
	Fe	2.77	2.65	2.33	1.38
95% OPC + 5% RHA 30k ppm Fe	Ca	48.93	49.03	50.13	52.15
	O	23.47	22.76	17.65	18.45
	Si	17.37	18.19	19.23	20.19
	Fe	2.53	2.44	2.29	2.05

*N/A = Not Available

APPENDIX F: ICP-OES Results of Leachate (Iron)

Sample		Concentration of Fe in Leachate (ppm)								
		Contact Duration (hour)								
	Triplicate	1	4	7	14	24	96	168	336	672
100% OPC + 10k ppm Fe	1	1.679	1.992	1.837	2.257	1.373	1.075	0.379	0.262	0.093
	2	1.756	1.831	1.811	2.111	1.625	0.814	0.525	0.186	0.097
	3	1.607	2.131	2.616	2.118	1.188	0.687	0.518	0.276	0.105
	Avg	1.681	1.985	2.088	2.162	1.395	0.859	0.474	0.241	0.098
95% OPC + 5% RHA 10k ppm Fe	1	1.066	1.361	1.295	1.361	1.306	0.708	0.345	0.193	0.059
	2	1.391	1.216	1.458	1.509	1.254	0.618	0.306	0.174	0.051
	3	1.145	1.668	1.565	1.453	1.324	0.675	0.314	0.196	0.034
	Avg	1.201	1.415	1.439	1.441	1.295	0.667	0.322	0.188	0.048
100% OPC + 30k ppm Fe	1	2.315	2.537	3.516	4.545	3.537	2.885	1.989	1.284	0.795
	2	1.682	3.991	3.905	4.126	3.846	2.962	2.329	1.316	0.754
	3	2.365	3.589	4.011	4.365	3.589	2.715	2.539	0.868	0.691
	Avg	2.121	3.372	3.811	4.345	3.657	2.854	2.286	1.156	0.747
95% OPC + 5% RHA 30k ppm Fe	1	1.878	2.893	3.237	3.347	2.883	1.835	1.379	0.964	0.464
	2	1.957	2.631	3.018	3.521	2.833	1.814	1.425	0.891	0.495
	3	1.907	2.734	3.019	3.538	2.778	1.897	1.318	0.984	0.484
	Avg	1.914	2.753	3.091	3.469	2.831	1.849	1.374	0.946	0.481

APPENDIX G: ICP-OES Results of Leachate (Calcium)

Sample		Concentration of Ca in Leachate (ppm)								
		Contact Duration (hour)								
	Triplicate	1	4	7	14	24	96	168	336	672
100% OPC + 0k ppm Fe	1	938.20	1483.00	1687.00	1755.00	1954.00	1665.00	1639.00	1627.00	1405.00
	2	956.60	1475.00	1882.00	1722.00	4030.00	1823.00	1823.00	1573.00	1648.00
	3	889.00	1295.00	1503.00	1478.00	2060.00	2422.00	2422.00	1654.00	1656.00
	Avg	927.93	1417.67	1690.67	1651.67	2681.33	1970.00	1961.33	1618.00	1569.67
95% OPC + 5% RHA 0k ppm Fe	1	861.70	1471.00	1535.00	1470.00	1555.00	1494.00	1339.00	1962.00	1019.00
	2	798.10	1357.00	1454.00	1473.00	1563.00	1525.00	1341.00	1233.00	1284.00
	3	2631.00	1459.00	1399.00	773.30	1531.00	1457.00	1330.00	1236.00	1090.00
	Avg	1430.27	1429.00	1462.67	1238.77	1549.67	1492.00	1336.67	1477.00	1131.00
100% OPC + 10k ppm Fe	1	944.60	1678.10	1705.10	1961.30	1923.20	1800.50	1785.60	1549.30	1298.40
	2	1088.90	1673.40	1818.30	1795.40	1904.50	1878.40	1648.20	1599.40	1297.60
	3	1019.60	1657.20	1624.90	1877.40	1955.10	1778.20	1624.50	1690.30	1329.20
	Avg	1017.70	1669.57	1716.10	1878.03	1927.60	1819.03	1686.10	1613.00	1308.40
95% OPC + 5% RHA 10k ppm Fe	1	935.20	1433.20	1557.30	1633.80	1734.50	1574.30	1559.40	1198.60	1155.90
	2	877.40	1299.30	1622.30	1555.80	1755.40	1597.90	1466.80	1388.40	1099.40
	3	964.20	1492.30	1563.10	1611.30	1666.50	1584.70	1496.70	1324.80	1096.70
	Avg	925.60	1408.27	1580.90	1600.30	1718.80	1585.63	1507.63	1303.93	1117.33
100% OPC + 30k ppm Fe	1	929.10	1566.40	1788.40	1811.30	1877.60	1800.90	1556.50	1456.30	1299.50
	2	978.30	1455.90	1698.40	1799.30	1747.20	1724.30	1518.90	1422.60	1280.30
	3	910.80	1613.50	1867.40	1825.60	1805.30	1729.40	1600.50	1459.90	1199.20
	Avg	939.40	1545.27	1784.73	1812.07	1810.03	1751.53	1558.63	1446.27	1259.67
95% OPC + 5% RHA 30k ppm Fe	1	807.80	1305.60	1299.30	1488.20	1627.90	1567.40	1489.50	1213.50	856.20
	2	769.30	1206.40	1628.90	1563.90	1677.80	1566.80	1477.80	1198.70	1022.30
	3	799.90	1300.50	1512.10	1523.90	1649.30	1499.40	1353.70	1159.60	973.20
	Avg	792.33	1270.83	1480.10	1525.33	1651.67	1544.53	1440.33	1190.60	950.57

APPENDIX H: pH value of Leachate

Sample	Triplicate	Contact Duration (hour)								
		1	**4**	**7**	**14**	**24**	**96**	**168**	**336**	**672**
100% OPC + 0k ppm Fe	1	4.61	4.91	5.04	5.12	6.91	11.58	9.72	9.02	10.64
	2	4.67	4.74	5.25	5.29	8.37	11.69	8.62	8.77	10.74
	3	4.68	4.92	5.51	5.41	5.67	11.71	8.64	8.85	10.79
	Avg	**4.65**	**4.86**	**5.27**	**5.27**	**6.98**	**11.66**	**8.99**	**8.88**	**10.72**
95% OPC + 5% RHA 0k ppm Fe	1	4.47	5.48	6.26	6.25	11.31	11.68	11.74	11.47	7.16
	2	4.44	5.49	5.31	7.31	11.41	11.71	11.97	11.61	7.07
	3	4.58	5.38	5.64	5.85	9.43	12.03	11.66	11.39	7.21
	Avg	**4.50**	**5.45**	**5.74**	**6.47**	**10.72**	**11.81**	**11.79**	**11.49**	**7.15**
100% OPC + 10k ppm Fe	1	4.51	5.22	6.23	8.21	8.48	10.88	9.99	11.41	11.59
	2	4.56	5.13	5.92	7.99	8.52	10.81	10.88	11.23	11.61
	3	4.58	5.22	5.88	7.25	8.53	10.88	10.10	11.52	11.52
	Avg	**4.55**	**5.19**	**6.01**	**7.82**	**8.51**	**10.86**	**10.32**	**11.39**	**11.57**
95% OPC + 5% RHA 10k ppm Fe	1	4.52	5.35	5.35	6.33	7.83	10.73	9.85	11.23	11.21
	2	4.53	5.44	5.55	7.03	7.92	10.72	9.62	11.34	11.29
	3	4.54	5.41	5.43	7.51	7.79	10.92	9.89	11.54	11.11
	Avg	**4.53**	**5.40**	**5.44**	**6.96**	**7.85**	**10.79**	**9.79**	**11.37**	**11.20**
100% OPC + 30k ppm Fe	1	4.55	5.02	6.13	7.04	10.68	10.53	9.44	11.49	11.09
	2	4.52	5.12	6.22	6.99	9.46	10.32	9.67	11.21	10.99
	3	4.53	5.17	6.09	6.75	10.34	10.52	9.11	11.37	10.93
	Avg	**4.53**	**5.10**	**6.15**	**6.93**	**10.16**	**10.46**	**9.41**	**11.36**	**11.00**
95% OPC + 5% RHA 30k ppm Fe	1	4.35	4.96	5.82	6.89	7.77	10.67	9.56	11.42	11.32
	2	4.22	4.77	6.02	6.77	7.34	10.66	8.66	11.44	11.32
	3	4.27	5.02	5.59	6.25	7.45	10.76	9.15	11.52	11.34
	Avg	**4.28**	**4.92**	**5.81**	**6.64**	**7.52**	**10.70**	**9.12**	**11.46**	**11.33**